工 學 碩 士 學 位 論 文

Synthesis and Spectral Characteristics of Biquinoline and Diazepine

2015 年 2 月

釜 慶 大 學 校 大 學 院

印 刷 工 學 科

麻 勇

工 學 碩 士 學 位 論 文

Synthesis and Spectral Characteristics of Biquinoline and Diazepine

指導敎授　孫 世 模

이 論文을 工學碩士 學位論文으로 提出함.

2015 年 2 月

釜 慶 大 學 校 大 學 院

印 刷 工 學 科

麻 勇

Contents

List of Figures

List of Tables

List of Appendixes

Biquinoline 및 Diazepine 합성 및 분광특성

YONG MA

부경대학교대학원 인쇄공학과

요약

OLED 는 신형평판디스플레이로써 낮은 전력소모, 자체발광, 고체상태의 구조, 높은 발광률, 넓은 시야각, 유연성 등 이점을 가지고 있어, 현재 활발한 연구가 진행되고있다.

근래, 유기전자를 기초로 한 반도체 재료가 관심을 받고 있으며, 특히 N-Heterocyclic 를 가진 재료가 큰 관심을 받고 있다. 비쌍극 구조인 질소원자의 특성으로 하여 n-형 또는 p-형 반도체 재료를 얻을 수 있다. 이런 형식의 재료는 OLED 의 개발에 큰 잠재력을 가지고 있다.

Quinoline 과 diazepine 을 가진 화합물은 열안정성, 높은 기계강도와 산화 방지성 등 전기적, 광학성 성질을 가지므로 OLED 재료 중 전자수송 재료로 연구되고있으나, 쉽게 합성되지 않는 단점을 가지고있다.

본 논문에서는 biquinoline 과 이의 이성질체를 모체로 한 9,9-dimethyfluorene 과 N-phenylcarbazole 를 치환기로 하여 Suzuki 반응을 통해 네가지 화합물을 합성하였다. 또 diazepine 을 모체로 thiophene 과 furan 을 치환기로 하여 Suzuki 반응을 통한 두가지 화합물을 합성하였다. 그런다음 HNMR, GC-MS 와 HPLC 로 정성분석하였다.

UV-Vis Absorption spectrum (Abs), Photoluminescence (PL), Differential Scanning Calorimetry (DSC), Cyclic Voltammetry (CV) 방법으로 6 가지 화합물의 광학, 전자학 특성을 측정하여 최대 흡광과 발광 파장, cut off wavelength, 유리계 온도전환과 용해점, 밴드 갭 (Eg), HOMO, LUMO 등 중요한 데이터를 얻었다. 이 데이터를 기초로 제일 적합한 유기 전자수송 화합물을 예측할 수 있다.

키워드: 평판디스플레이, 반도체재료, 전자수송재료

1. Introduction

1.1 OLED research and development

Nowadays the world is experiencing unprecedented historic change, economic globalization is an inevitable trend of world economic development and its fundamental principle is the globalization of information. It is not only a significant connection among people, and also prompt people to get the worldwide information resources. It makes globalized markets become increasingly open, syncretic and continue to promote the progress of mankind.

Display technology as the most important medium of information industry plays an unshakable role in the social production and people's daily life. It is crucial for the information display device between human and media information. With the rapid development of the information society, people also put higher requirements forward displaying materials. Initially Cathode Ray Tube (CRT) is used as TV and image display device, but its drawbacks are bulky, heavy, low energy utilization and complex manufacturing process. With the development of the times, the Flat Panel Display (FPD) technology develops rapidly, its output value has exceeded CRT. Now the most popular FPD is Liquid Crystal Display technology (LCD). LCD has many advantages, such as small size, thin, light weight, image no flicker, no radiation and low energy consumption, but it also has fatal flaws, such as limited Visual range, not long-term use, large temperature impact, slow response, etc.

Organic Light-emitting Diode (OLED) is made of an organic material film. It achieves light-emission and display by current driving to organic semiconductor thin film. OLED as a new flat panel display technology has its merits, such as all solid, fast response, high brightness, low driving voltage, flexible curl, super lightweight and simple production process, etc.[1,2] OLED are currently classified into two groups according to the type of emissive layer. One class of light emissive films is formed from low-molecular materials and prepared by a dry process such as vacuum evaporation coating. The other class of films is polymer, prepared by wet process such as spin- or dip-coating.[3-6] These qualities make OLED become a hotspot in photoelectrochemistry and material science field in recent years. And it is one of the highly

competitive researches in international Display technology nowadays. OLED is known as the 21st Century's most promising next-generation display devices.

OLED exploration was originated in the 1950s, Andr é Bernanose and co-workers applied organic material to prepare organic electroluminescent device. In the 1960s, New York University professor Martin Pope and co-workers firstly discovered and reported the blue luminescence of organic small molecule material crystal anthracene under hundreds of volts.[7] This work opened the prelude to an organic electroluminescent study. In 1982, Vincelt.P. S. and co-workers firstly prepared OLED by the vacuum vapor deposition.[8] This study makes the preparation of large-area organic electroluminescent devices possible. In 1987, Ching W. Tang and Steven Van Slyke reported a stacked EL cell structure tris(8-hydroxyquinoline) aluminum (Alq_3), which has a luminous efficiency of 1.5lm/W and a luminance of 1000cd/m^2 for green light under lower operating voltage than 10V.[9] This work makes organic electroluminescence phenomenon of great concern by national researchers, since then a new chapter in the history of OLED research was launched. Research of polymer electroluminescence culminated in 1990 with J. H. Burroughes et al. at the Cavendish Laboratory in Cambridge reporting a high efficiency green light-emitting polymer based device using 100 nm thick films of poly(p-phenylene vinylene).[10] It opened up another important field of organic electroluminescent devices. Thereafter in 1992, the University of California D. Braun and A. J. Heeger used plastic as a substrate to prepare a flexible display, making OLDE showing its fantastic flexible display characteristics.[11] In 1997, Forrest discovered and reported in a red phosphorescent organic light-emitting phenomenon of the fluorescent dye.[12] Phosphorescent device which is theoretically the internal quantum efficiency can reach 100%, the device efficiency is greatly improved.

After decades of development, because the organic electroluminescent material has many advantages, such as low-voltage DC drive, high brightness, high efficiency, low cost, easy to implement full-color large-area display, is used in industrial, military, medical and many other fields.

Comparing to phosphorescent materials and polymer luminescent material, organic small molecules light-emitting materials research start early and relatively mature. After twenty years of development, small molecule OLED flat panel display technology has begun to enter

the industrial stage, and many products are manufactured.

Currently, the study of OLED are mainly concentrated on the improvement of the performance of the device efficiency and lifetime, and find some new type of organic electroluminescent materials. For examples, optimizing the production process, using flexible transparent electrode, designing multilayered OLED device structure and exploring its mechanism of attenuation. Furthermore a number of high luminous efficiency and excellent heat stability of small molecule organic electroluminescent or polymer material is needed to explore and synthesize.

1.2 OLED related knowledge

1.2.1 OLED structure

Currently, the most common method for preparing OLED is a sandwich type structure. The electrodes are added in both sides of the light-emitting layer, and a transparent electrode is added in its one side to obtain a surface-emitting. OLED film formation temperature is low. The anode is typical ITO glass. The light-emitting layer is deposited on the ITO by vapor deposition method or a spin coating method. After the preparation of a single-layer or multi-layer organic thin film, the metal cathode is deposited on the film by vapor deposition. According to the function of organic thin film, OLED device structure can be divided into single, double, triple and multi-layer structure.

Because single-layer structure OLED is difficult to overcome many shortcomings, so at present most of the OLED devices are prepared by using multi-layer film structure. The initial multi-layer device is a double-layer device that contains a hole-transport layer. In a double-layer device, the light-emitting layer is used to not only emit light, but also transport electrons. Introduction of a hole-transport layer has largely solved the injection imbalance between electron and hole. It also has improved the I-V characteristics of the device, so the luminous efficiency of the device is greatly enhanced. Thus, the nature of the light-emitting layer determines the specific structure of the device. When the light-emitting layer material can transport both holes and electrons, or its transporting ability to holes and electrons are low,

generally the triple-layer structure is required. Such a device structure can be able to make three layers of organic material simultaneously and to promote material selection and optimizing device performance. Thus currently OLED multi-layer structure is often used.[13-15]

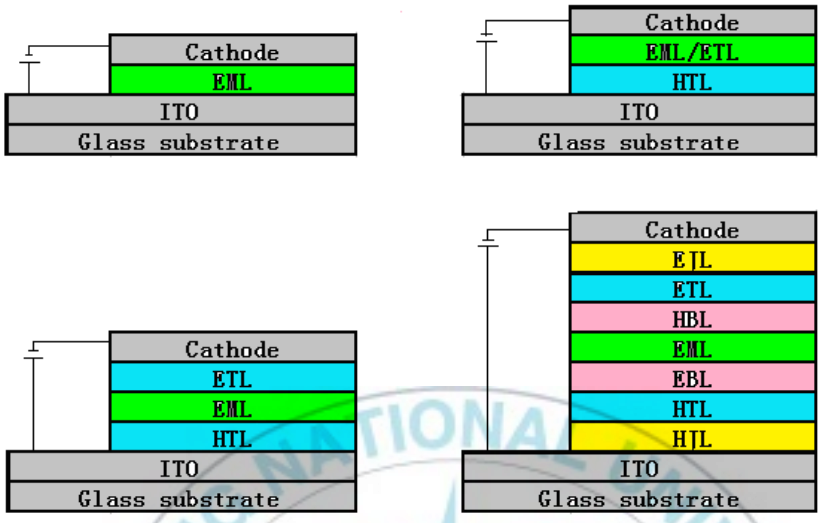

EIL--electron injection layer HIL--hole injection layer

ETL--electron transport layer HTL--hole transport layer

EBL--electron blocking layer HBL--hole blocking layer

EML--light emitting layer

Figure 1. OLED structures

With the continuous development of OLED, the device structure design has become even more complicated. It evolves from simple double-layer structure to a multi-layer structure and from host emitting to the doping host-guest system.[16,17] Each functional layer is also increasingly refined. Preparation of single-layer devices is economical and convenient, but most of the organic materials are the most efficient to only one of carrier transports. A material is difficult to match the Fermi level of both anode and cathode at the same time, so single-layer device has some problems: carrier injection imbalance, exciton easily quenching, low luminous efficiency, etc. An electron-transport layer, a light-emitting layer and a hole-transport layer, meanwhile they are introduced the device. These greatly reduce the starting voltage of the device and improve the efficiency of the device. In order to control the

holes and electrons in the light-emitting layer needs to introduce different functional layers, such as hole-injection layer, electron-blocking layer, hole-blocking layer, electron-injection layer, etc. However, this approach has led to an increase in the number of layers, the device fabrication is relatively more complex, which hinders the process of industrialization and increases the economic cost. Therefore, the rational design of device structure to improve the device performance is extremely important. To achieve OLED industrialization must explore the economical, convenient and reasonable preparation process.

1.2.2 OLED basic principle

Organic electroluminescence is a process that electrical energy transforms into light energy. OLED is a light-emitting diode with injection of carriers, namely under the applied voltage holes injected from the anode and electrons injected from the cathode encounter to form excitons in the organic light-emitting layer. Recombined excitons transfer energy to the light-emitting layer, organic light-emitting molecules are excited and transited from the ground state to the excited state. When excited molecules transits from its excited state back to the ground state, radiation transition occur resulting luminescence. The organic electroluminescence process generally includes five stages:

(1) Carriers injection:

Carriers injection and transport process are the most basic process of organic electroluminescence. Carriers injection is under the applied DC electric field, electrons and holes are injected into the organic functional layer from the cathode and the anode of the device.

(2) Carriers migration:

The injected holes and electrons migrate to the organic light-emitting layer from the hole-transport layer and electron-transport layer, respectively.

(3) Carriers recombination:

Holes and electrons combine to form excitons.

(4) Excitons migration:

Under the influence of an external electric field, the excitons decay and transfer energy to the organic light-emitting molecules. Electrons of light-emitting molecule orbit transit from

the ground state to the excited state.

(5) Electroluminescence:

When excited electrons of organic light-emitting molecule transit from its excited state back to the ground state, radiation transition occurs. Produce photons and release light energy.

OLED exciton generation process is different to photoluminescence. In electroluminescence, carriers are injected from opposite electrodes, and combine at a proper position of the device through the electron-transport layer and the hole-transport layer to form excitons. The triplet state is formed in the system not only through intersystem crossing between singlet states, but also through a different spin configuration. Namely in electroluminescence, generated excitons can be either a singlet state or a triplet state. Because it is inhibited spinning between triplet states, so in the conventional EL devices triplet states luminescence is invalid, its photoelectric conversion efficiency is only 25%. The organic electroluminescent device has a low luminous efficiency is a key constraint factor in the application of the device. How to improve the luminous efficiency by triplet state has very great significance for OLED.[18]

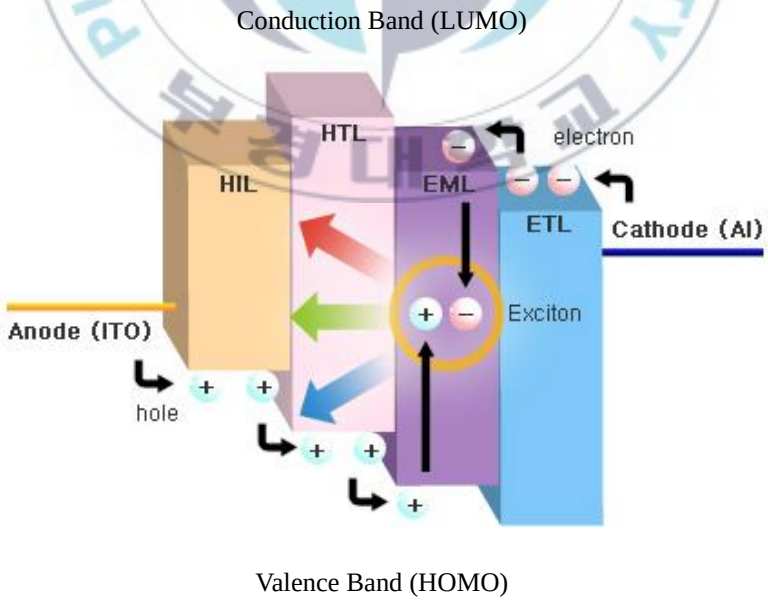

Figure 2. OLED emission process

1.2.3 OLED preparation

The main purpose is that the preparation of organic electroluminescent device is to reach the nano-scale film thickness with organic electroluminescent material. Currently the more common and mature methods include vacuum evaporation coating, spin coating and ink-jet printing, etc. When using these methods, you must ensure that the environment clean and dust-free.

Organic small molecule light-emitting material, organic metal complex and metal electrode mainly apply to vacuum evaporation coating method to prepare film.[19] This method needs to use a vacuum evaporation coating equipment with very high vacuum degree. This method has a very high requirement to the equipment, the forming film process must be carried out under high vacuum, the quality of the forming film depends on the vacuum degree. Spin coating method and ink-jet printing method are suitable for organic small molecule material or polymeric molecule material with good solubility. Spin coating method is a procedure used to deposit uniform thin films to flat substrates. Usually a small amount of coating material is applied to the center of the substrate, which is either spinning at low speed or not spinning at all. The substrate is then rotated at high speed in order to spread the coating material by centrifugal force. A machine used for spin coating is called a spin coater, or simply spinner. Rotation is continued while the fluid spins off the edges of the substrate, until the desired thickness of the film is achieved. The applied solvent is usually volatile, and simultaneously evaporates. The thickness of the film also depends on the Viscosity and concentration of the solution and the solvent. The film prepared in this way is uniform, pinhole-free, low requirements for the equipment, and without excessive material, simple and convenient operation, it is beneficial to realize large-scale preparation of OLED. The ink-jet printing method is a new OLED preparation method. This method is easy to implement panchromatic and color display and to achieve the manufacture of large size OLED, low manufacturing cost, it greatly promotes large-scale production of OLED.

1.3 OLED materials

According to the different functions of material, it is classified into light-emitting material, carrier material, electrode material, etc. According to the molecular structure of material, it is classified into organic small molecule materials and polymer materials. In recent years, researchers have already invested a lot of effort in order to find the excellent performance of organic electroluminescence materials.

1.3.1 Organic small molecule electroluminescent materials

Organic light-emitting materials should have some features, such as excellent thermal stability and chemical stability, higher fluorescence quantum efficiency, good plasticity and better light stability.

Compared with the polymer light-emitting material, an organic small molecule light-emitting material has the following advantages:

(1) Easily purified by vacuum sublimation, recrystallization, column chromatography, etc. Since the purity is very important in the OLED. When the purity of material is higher, the luminescence quenching chance is lower, luminous efficiency and lifetime of the device are improved. So this makes the small molecule materials have certain advantages.

(2) Organic small molecules used in the method of vacuum evaporation coating to form a dense film with no impurities. On the contrary, the polymer material due to their molecular properties, the film should not use the vacuum evaporation coating, usually use the spin coating. In the preparation of the multilayer film structure, because of the solvent, it often leads to changes in membrane shape or even destroy the previous layer, thus the effectiveness of the device is affected. Therefore, when preparing a multi-layer structure device, the small molecule has its own advantages. In particular, in the preparation of the lattice and multicolor OLED devices, these advantages are particularly prominent.

1.3.1.1 Organic small molecule red emitting materials

Since 1989, Deng Qingyun used DCM1 and DCM2 as a guest in the light-emitting material doped in Alq_3, and achieve efficient organic red emitting devices. DCM series of red

emitting materials have been widely used in OLED. Currently, more commonly used red emitting material is mainly DCJTB.[20] In contrast with DCM series compounds, the synthesis and purification of the compound is simple, the red emitting quality is good.

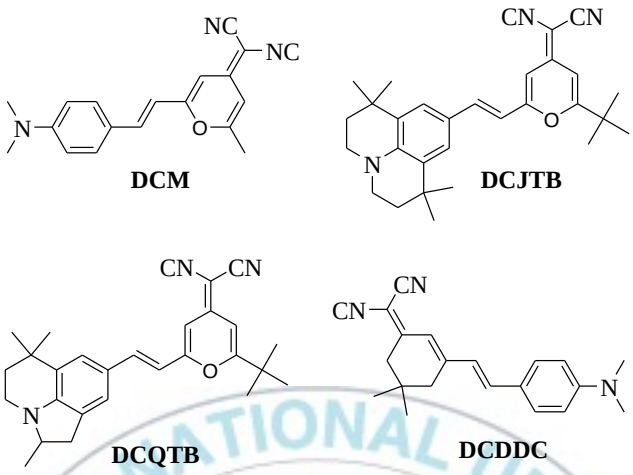

Figure 3. Classical red emitting OLED materials

1.3.1.2 Organic small molecule green emitting materials

Small organic molecule green emitting materials mainly include: coumarin dyes (Coumarin6), quinacridone dye (QA),[21] other species such as a hole transport capabilities of carbazole derivatives, organic silicon compound, pyrazolo quinoxaline derivatives, diaminoanthraquinone derivatives (α-NPA), coronene, imidazole derivatives, thiophene pyrrole and naphthalimide etc.

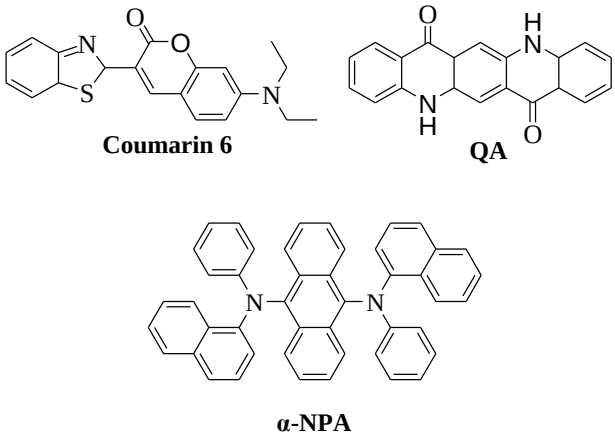

Figure 4. Classical green emitting OLED materials

1.3.1.3 Organic small molecule blue emitting materials

The blue emitting material is the issue of organic electroluminescent research all along. In order to achieve a stable and effective blue emission, the designed molecular chemical structure must have a degree of conjugation. Many fully conjugated and partially conjugated small molecule compounds have been developed, but the blue emitting materials can be used in OLED is very limited. The blue emitting materials must have a wider Band gap, and its electron affinity must be matched with the first ionization energy. An inorganic blue emitting material is difficult to obtain.

At present, the blue emitting materials include: hetero atom-free aromatic compounds, aromatic amines, organic boron compounds, organic silicon compounds etc. First discovered and used single-crystal anthracene in EL device is blue-light material. However, since the anthracene easily crystallizes, it is difficult to form the amorphous film. To avoid crystallization and to improve its thermal stability, many anthracene-based compounds have been developed and show a good performance of the blue-light.[22,23] In addition, fluorenes, spirofluorenes,[24] aromatic amines, diphenyl vinyl aryl compounds and organic silicon compounds are better blue-light materials.

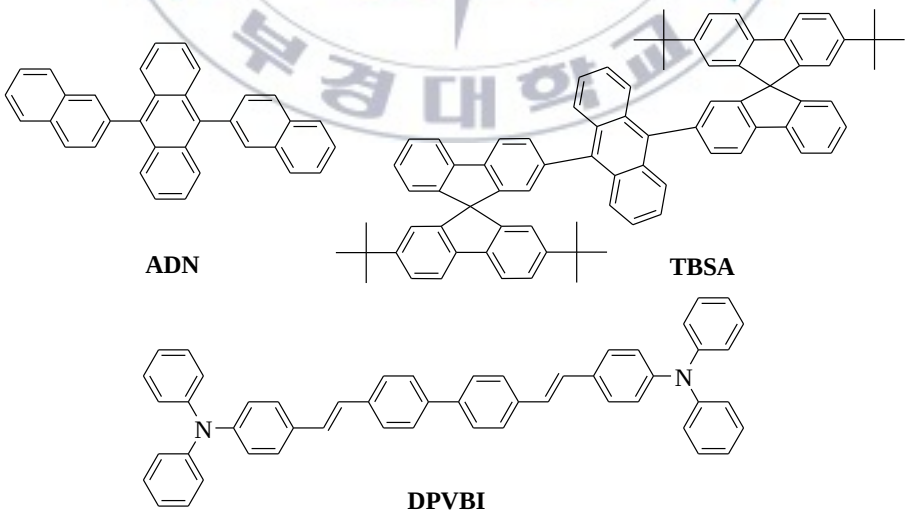

Figure 5. Classical blue emitting OLED materials

1.3.2 Carrier materials

The carrier materials include to a carrier injection material and a carrier transport

material. According to its function, it includes to a hole-injection material, a hole-transport material, an electron-transport material and a hole-blocking material.

1.3.2.1 Hole-injection materials

The hole-injection material can reduce the interfacial barrier between ITO electrode and the hole-transport layer, but also improve the degree of adhesion, increase the hole-injection contact, balance hole and electron injection.[25]

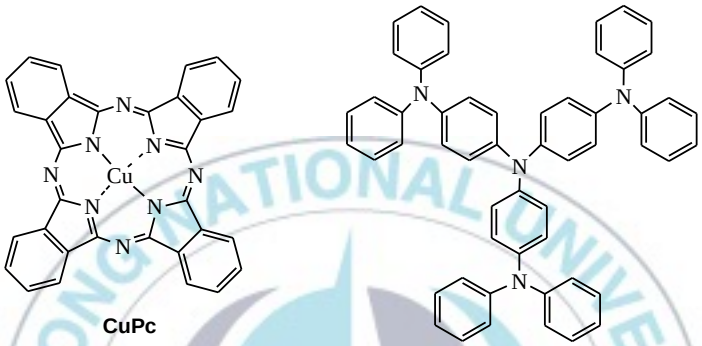

Figure 6. Classical hole-injection materials

1.3.2.2 Hole-transport materials

The hole-transport material should have a strong electron-donating property. More smaller interfacial barrier is between the hole-transport and the anode, more better the stability of the device is.

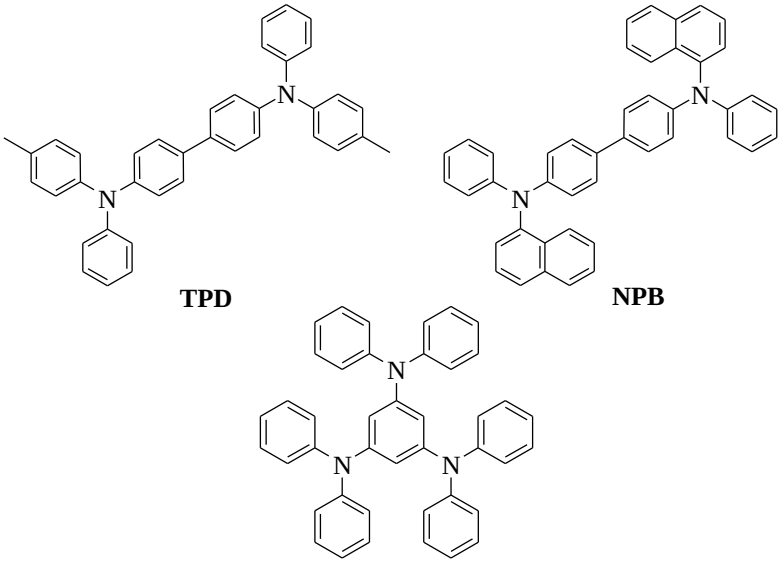

Figure 7. Classical hole-transport materials

1.3.2.3 Hole-blocking materials

In order to injected electrons and holes can well form excitons in the light-emitting layer and emit light, it often needs use the hole-blocking material in the organic light-emitting device to block the holes into the electron-transport layer. Such materials generally have a lower HOMO, so as to effectively prevent the transmission of holes, the recombination of excitons in the light-emitting layer instead of the electron-transport layer.[26,27]

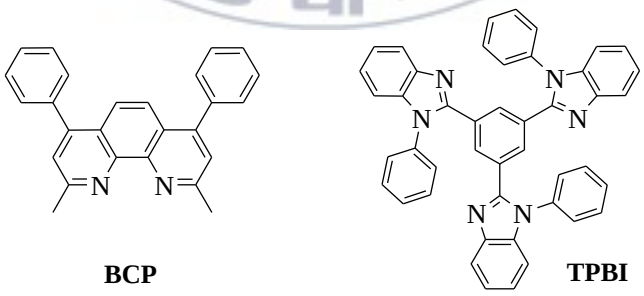

Figure 8. Classical hole-blocking materials

1.3.2.4 Electron-transport materials

The electron-transport material occupies a considerable position in OLED. The electron-transport material on the molecular structure should be an electron-defect system. An excellent electron-transport material should have the following characteristics:

(1) Reversible electrochemical reduction and enough high reduction potential, thereby forming a stable anion;

(2) Appropriate HOMO and LUMO value, thereby electrons injected from the cathode with a minimum barrier;

(3) Higher electron mobility, thereby recombination zone away from cathode and increasing excitons generation rate;

(4) High thermal stability and glass transition temperature (T_g);

(5) Excellent film-forming property.

According to the molecular structure, organic electron-transport materials can be divided into:

(1) Arylene diimide. It includes to perylene-3,4,9,10-tetracarboxylic acid bisimides, PBIs) and its derivatives, naphthalene-1,8,4,5-tetracarboxylic diimides, NDIs) and its derivatives, rod-like benzene, naphthalene, anthracene, tetracene, pentacene diimides and their derivatives. They not only have excellent electron-transport characteristic, but also have a high molar extinction coefficient, Visible-near infrared absorption rang, excellent optical, electrical, thermal stability. Therefore, these materials are widely used in the organic electron-transport field.

(2) Fullerene and its derivatives. It includes to $PC_{61}BM$ and $PC_{71}BM$. They have a strong electron-accept ability, mainly in their lower and triply-degenerated LUMO and accepting six electrons.

(3) Organic electron-transport materials containing electron-withdrawing group (halogen (F, C_nF_{2n+1}), cyano (CN)), such as perfluoro-substituted oligothiophene.

(4) A acceptor of the p-type electron-transport donor-acceptor structure as the core of small molecule organic electron-transport material, such as benzothiadiazole as the core of a n-type electron-transport material.

(5) Organic electron-transport materials containing a metal (Cu, Al, Ru, Zn) of organometallic complexes, such as Alq_3 and sixteen fluorine-substituted copper phthalocyanine ($F_{16}CuPc$).

(6) Organic conjugated polymers.

(7) Quinoline derivatives.

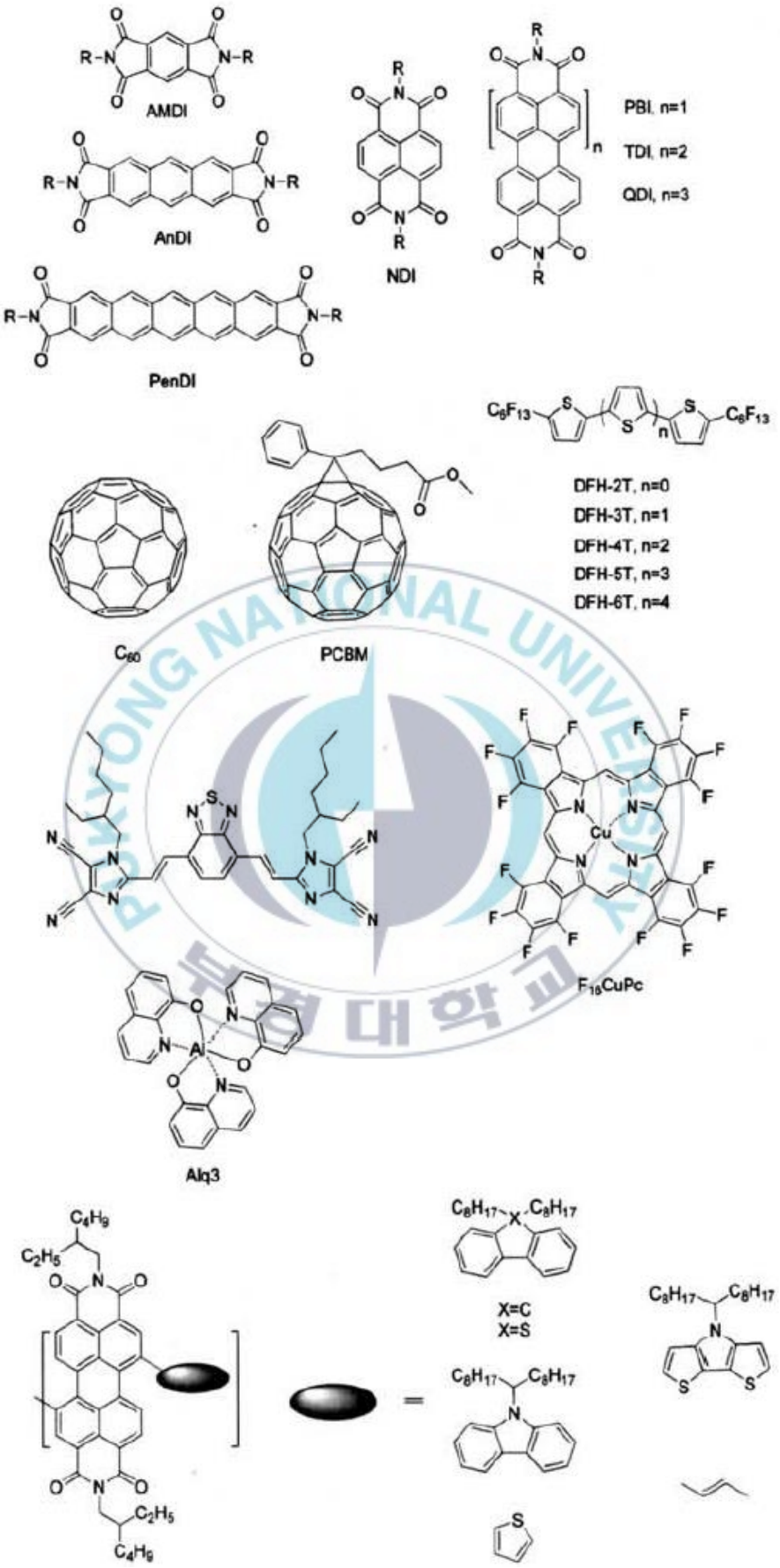

Figure 9. Structures representation of organic electron-transport materials

1.3.2.5 Electron-transport materials base on quinoline

Quinoline has an electron-defect molecular structure. It is widely used in the electron-transport layer of OLED.

(1) Polyquinoline: Poly(2,2'-(p-phenylene)-6,6'-bis(4-(p-tert-butylphenyl)quinoline)),[28] polyquinolines containing a 9,9-di-n-hexylfluorene unit in the main chain,[29] polyquinolines containing a 9,9'-spirobifluorene unit in the main chain,[30] poly{[2,2'-bis-(4-phenylquinoline)-1,4-phenylene]-alt-phenoxy}.[31]

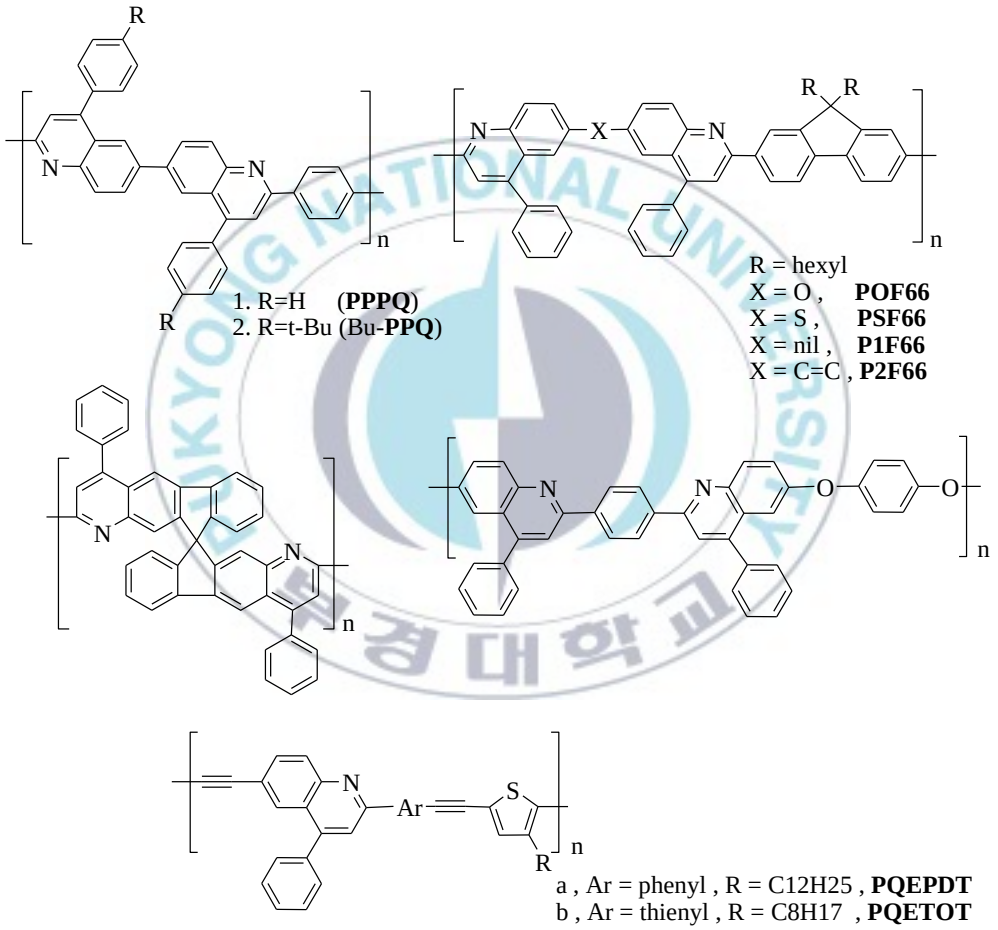

Figure 10. Five polyquinoline organic electron-transport materials

(2) Small molecule quinoline:

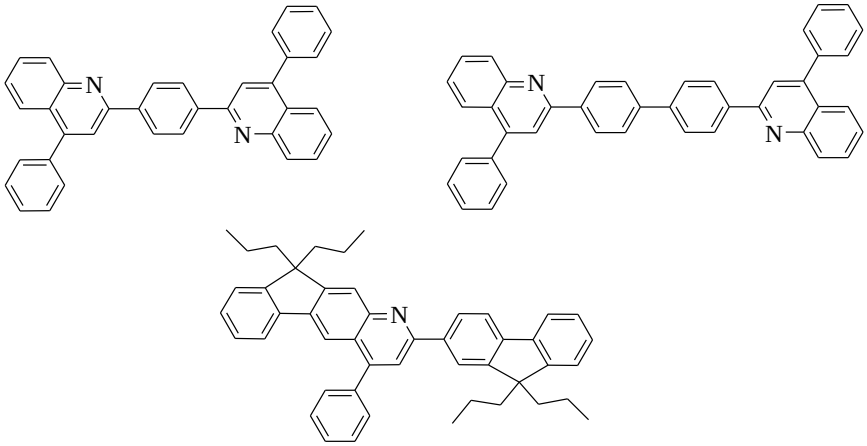

Figure 11. Three small molecule quinoline organic electron-transport materials

1.4 Purpose of this research

Organic electronics based on semiconducting materials has attracted much interest in recent years. N-Heterocyclic based materials having electrically conducting properties are of particular interest. Depending on the nature of incorporation of the nitrogen atom in the monomer unit, either p- or n-type semiconducting materials are obtained. However they are not readily synthesized and examples include the compound classes like oxadiazoles,[32] quinoxalines,[33] pyridines,[34] carbazoles,[35] quinolines, benzimidazoles,[36] benzothiadiazoles,[37] and bis(benzothiadiazole)s.[38] The donor–acceptor type materials based on these classes have shown potential for use in OLED.[39]

Quinoline and diazepine based materials have been widely studied for applications as electron-transport material in OLED due to their electronic and optical properties.[40] Polyquinolines possess n-type electrically conducting properties along with good thermal, mechanical, and oxidative properties. There are many reports on quinoline and diazepine based polymers but limited work has been done on biquinoline and diazepine based small moleculars.[41,42]

In this research, I have two purposes:

(1) Find a simple and fast route with a high yield to synthesize six biquinoline and diazepine derivatives.

(2) Through measuring and contrasting six synthesized compounds' optical characteristics, electrical characteristics and other characteristics, the more suitable organic electron-transport material will be obtained. It should have lower HOMO, LUMO value and higher Band gap value, high thermal and oxidative stability.

2. Experimental Section

2.1 Reagent

The following reagents used in the experiment are all from Aldrich Chemical Co., Inc.: 1,4-Dibromobenzene(98.0%), 4,4'-Dibromobiphenyl(98.0%), Furan(99.0%), 2-Bromo-9,9'-dimethyl-9H-fluorene(98.0%), 3-Bromo-9-benylcarbazole(98.0%), Benzaldehyde(97.0%), 2-Bromothiophene(98.0%), Bis(pinacolato)diboron(B_2Pin_2, 98.0%), Tetrakis(triphenylphosphine)palladium(0)($Pd(PPh_3)_4$, 99%), Bis(triphenylphosphine)palladium(II) dichloride($Pd(PPh_3)_2Cl_2$, 98%), Nitric acid(HNO_3, 99.5%), Tin powder(Sn, 99.8%, 325mesh), N-Bromosuccinimide(NBS, 99.0%).

The other reagents and solvents used in the experiment are all from Junsei Chemical Co., Ltd.: Copper powder(Cu, 99.7%, 200mesh), Iodine(I_2, 99.8%), Glycerol(95.0%), Potassium acetate(AcOK, 96.0%), Iron(II) sulfate heptahydrate($FeSO_4.7H_2O$, 98.5%), Sodium thiosulfate pentahydrate($Na_2S_2O_3.5H_2O$, 98.0%), Potassium carbonate(K_2CO_3, 98.0%), Sodium carbonate(Na_2CO_3, 98.0%), Hydrochloric acid(HCl, 35%), Sulfuric acid(H_2SO_4, 95%), Sodium hydroxide(NaOH, 96%), anhydrous Magnesium sulfate($MgSO_4$, 98.0%), Silica gel 60(0.063~0.200mm), Dichloromethane(MC, 95%), Methanol(MeOH, 95%), Ethanol(EtOH, 95%), Tetrahydrofuran(THF, 98%), Hexane(Hex, 95%), Ethyl acetate(EA, 95%), N,N-Dimethylformamide(DMF, 98%), 1,4-Dioxane(98%), tert-Butyl alcohol(t-BuOH, 95%).

2.2 Synthesis of compounds

2.2.1 Synthesis of compound 1 (5,5'-Di(9,9-dimethylfluorene-2-yl)-8,8'-biquinoline)

Compound 1 was prepared by using 1,4-Dibromobenzene as start material, via nitrification, condensation, reduction, Skraup synthesis, Suzuki coupling reaction.

2.2.1.1 Synthesis of 2,5-Dibromonitrobenzene

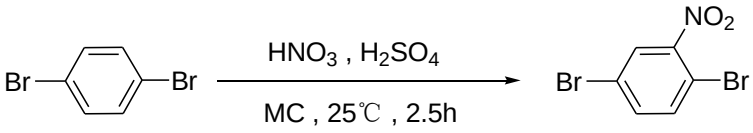

1,4-dibromobenzene 2,5-dibromonitrobenzene

A mixture of 99.5% Nitric acid (73g, 1153mmol) and 95% Sulfuric acid (294g, 2848mmol) was added dropwise to a solution of 1,4-Dibromobenzene (236g, 980mmol) in MC (500ml) at 25℃ for 1 hour. And the reaction mixture was stirred at 25℃ for 1.5 hour. The reaction mixture was diluted with ice water (2500ml), and extracted with MC (3×500ml). The combined organic layers were washed with water (3×700ml), dried over anhydrous $MgSO_4$, and distilled to dryness under vacuum. The crude was recrystallized from Ethanol to give pure product 251g (yield: 89%) as a light-yellow solid. m.p. 82-83℃, R_f=0.8 (SiO_2, EA: Hex=1:3), GC-Mass 280.9, $C_6H_3Br_2NO_2$, m/z (relative intensity): 280 (100%).

2.2.1.2 Synthesis of 4,4'-Dibromo-2,2'-dinitrobiphenyl

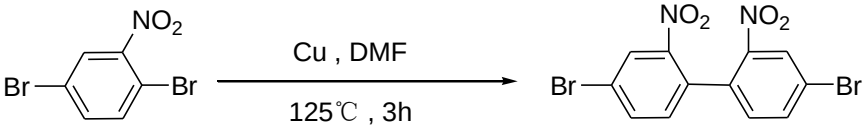

2,5-dibromonitrobenzene 4,4'-dibromo-2,2'-dinitrobiphenyl

To a stirring solution of 2,5-Dibromonitrobenzene (261g, 929mmol) in DMF (670ml) was added Copper powder (141g, 2220mmol), and the reaction mixture was heated to 125℃. After 3 hour, the mixture was allowed to cool to room temperature. The mixture was dissolved in MC (3000ml). The insoluble inorganic salts and excess copper were next removed by filtration through Celite. The filtrate was washed with water (5×1000ml), dried over anhydrous $MgSO_4$, and distilled to dryness under vacuum. The crude was recrystallized from EA to give pure product 124g (yield: 61%) as a yellow solid. R_f=0.6 (SiO_2, EA:

Hex=1:3), ^{1}HNMR (400MHz, $CDCl_3$): δ=7.17 (d, 2H), 7.84 (dd, 2H), 8.39 (d, 2H) ppm. GC-Mass 402.0, $C_{12}H_6Br_2N_2O_4$, m/z (relative intensity): 356 (100%).

2.2.1.3 Synthesis of 4,4'-Dibromobiphenyl-2,2'-diamine

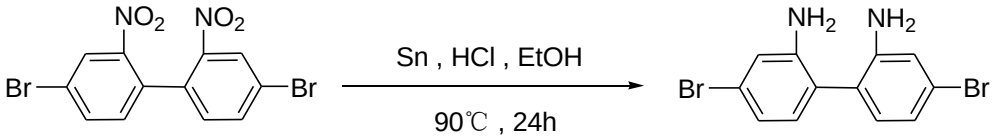

4,4'-dibromo-2,2'-dinitrobiphenyl　　4,4'-dibromobiphenyl-2,2'-diamine

To a solution of 4,4'-Dibromo-2,2'-dinitrobiphenyl (93.5g, 233mmol) in 1100ml of ethanol was added 35% w/w aqueous HCl (663ml). Tin powder (166g, 1398mmol) was then added portionwise over 1 hour, and the reaction mixture was heated to reflux at 90℃ for 24 hour. After cooling, the mixture was poured into ice water (2500ml) and then made alkaline with 30% w/w aqueous NaOH solution until the PH was 9.0. The product was next extracted with MC (3×1500ml) and the organic layer was washed with water (5×1000ml), dried over anhydrous $MgSO_4$, filtered, and then distilled to dryness under vacuum to give crude product 71.6g (yield: 90%) as a light-brown solid that can be used without further purification. R_f=0.5 (SiO_2, EA: Hex=1:3), ^{1}HNMR (400MHz, $CDCl_3$): δ=6.92 (s, 6H), 3.78 (s, 4H) ppm. GC-Mass 342.03, $C_{12}H_{10}Br_2N_2$, m/z (relative intensity): 342 (100%).

2.2.1.4 Synthesis of 5,5'-Dibromo-8,8'-biquinoline

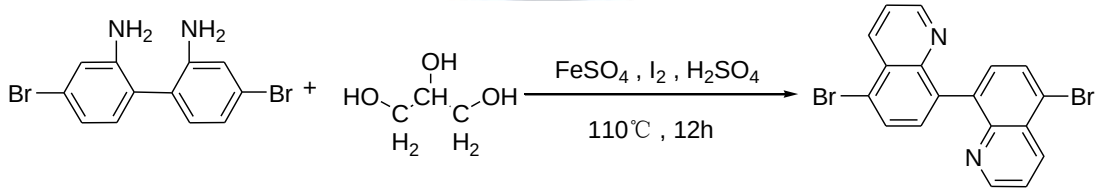

4,4'-dibromobiphenyl-2,2'-diamine　　glycerol　　5,5'-dibromo-8,8'-biquinoline

4,4'-Dibromobiphenyl-2,2'-diamine (18.5g, 54mmol), Glycerol (39.9g, 433mmol), Iron(II) sulfate heptahydrate (4.5g, 16mmol), Iodine (0.28g, 1.1mmol), and Sulphuric acid (83.3ml, 1486mmol) were taken in 500 ml round bottom flask and heated at 110˚C. The reaction progress was followed by TLC and after 12h was worked up. The cooled mixture was neutralized with NaOH and filtered, and the filter cake was dried at 70˚C under vacuum. The crude product so obtained was purified with silica gel chromatography and eluted with

(EA: Hex=1:6) as eluent. Product was recrystallized from (THF: Methanol=5:1) to give light-yellow solid 5.7g (yield: 25.5%). R_f=0.4 (SiO_2, EA: Hex=1:3), ^{1}HNMR (400MHz, $CDCl_3$): δ=8.79 (s, 2H), 8.66 (d, 2H), 7.99 (d, 2H), 7.63 (d, 2H), 7.5 (m, 2H) ppm. GC-Mass 414.09, $C_{18}H_{10}Br_2N_2$, m/z (relative intensity): 413 (100%).

2.2.1.5 Synthesis of 2-(4,4,5,5-Tetramethyl-1,3,2-dioxaborolan-2-yl)-9,9-dimethylfluorene

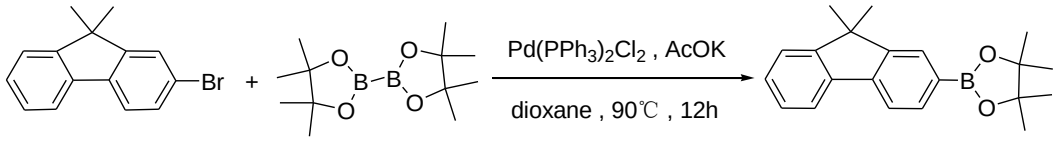

2-bromo-9,9-dimethyl-9H-fluorene bis(pinacolato)diboron

2-Bromo-9,9-dimethyl-9H-fluorene (27.3g, 100mmol), Bis(pinacolato)diboron (27.9g, 110mmol), $Pd(PPh_3)_2Cl_2$ (2.8g, 4mmol), Potassium acetate (39.3g, 400mmol) and 1,4-dioxane (400ml) were taken in 500 ml round bottom flask and heated at 90˚C under nitrogen. The reaction progress was followed by TLC and after 12h was worked up. The solvent 1,4-dioxane was distilled at 60℃ under vacuum. Then the residue was added into water (500ml) and extracted with MC (3×200ml) and the organic layer was washed with water (2×300ml), dried over anhydrous $MgSO_4$, filtered, and then distilled to dryness under vacuum. Then the residue was dissolved into hot EA, filtered, and distilled to dryness under vacuum to give crude product. The crude was recrystallized from Hexane to give pure product 28.9g (yield: 90%) as a light-yellow solid. R_f=0.8 (SiO_2, Hex). GC-Mass 320.23, $C_{21}H_{25}BO_2$, m/z (relative intensity): 320 (100%).

2.2.1.6 Synthesis of compound 1 (5,5'-Di(9,9-dimethylfluorene-2-yl)-8,8'-biquinoline)

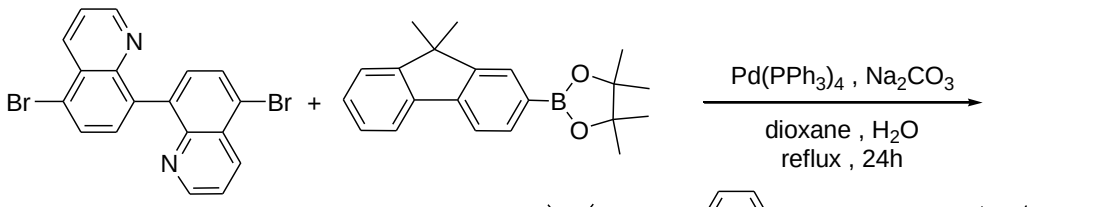

5,5'-dibromo-8,8'-biquinoline

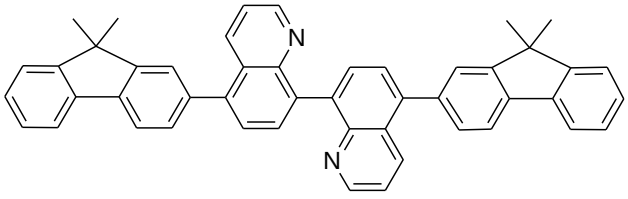

compound 1

5,5'-Dibromo-8,8'-biquinoline (1.2g, 2.9mmol), 2M Na_2CO_3 (8.7ml, 17.4mmol) and 2-(4,4,5,5-tetramethyl-1,3,2-dioxaborolan-2-yl)-9,9-dimethylfluorene (2.8g, 8.7mmol) were dissolved in 40ml of dioxane in a dried flask. The solution was purged with nitrogen for 20min, and then tetrakis(triphenylphosphine)palladium (0.2g, 0.174mmol) was added and the reaction mixture was refluxed (85℃) with stirring. The reaction progress was followed by TLC and after 24h was worked up. The cooled mixture was added into water (200ml), filtered and washed with Methanol. The crude product so obtained was purified with silica gel chromatography and eluted with (EA: Hex=1:1) as eluent. Product was recrystallized from (THF: Methanol=5:1) to give white solid 1.55g (yield: 83.5%, total yield: 10.4%). m.p. 336-337℃, R_f=0.3 (SiO_2, EA: Hex=1:3), ^{1}HNMR (400MHz, $CDCl_3$): δ=8.87 (d, 2H), 8.44 (d, 2H), 7.95 (d, 2H), 7.87 (d, 2H), 7.80 (d, 2H), 7.75 (d, 2H), 7.64 (d, 2H), 7.55 (d, 2H), 7.48 (d, 2H), 7.41-7.35 (m, 6H), 1.57 (s, 12H) ppm. $C_{48}H_{36}N_2$ 640.81.

2.2.2 Synthesis of compound 2 (5,5'-Di(9-phenylcarbazole-3-yl)-8,8'-biquinoline)

Compound 2 was prepared by using 1,4-Dibromobenzene as start material, via nitrification, condensation, reduction, Skraup synthesis, Suzuki coupling reaction.

2.2.2.1 Synthesis of 3-(4,4,5,5-Tetramethyl-1,3,2-dioxaborolan-2-yl)-9-phenylcarbazole

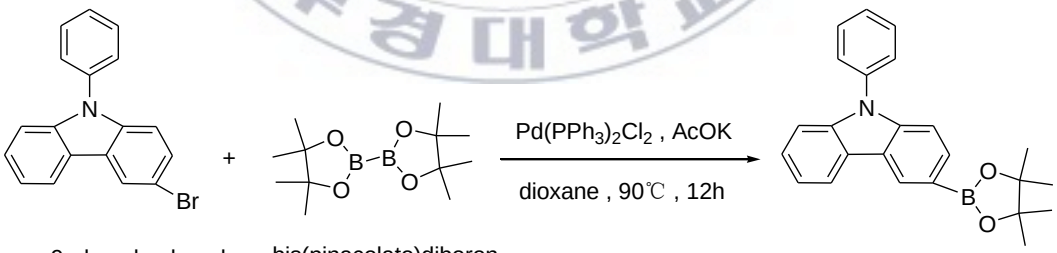

3-Bromo-9-phenylcarbazole bis(pinacolato)diboron

3-Bromo-9-phenylcarbazole (32.2g, 100mmol), Bis(pinacolato)diboron (27.9g, 110mmol), $Pd(PPh_3)_2Cl_2$ (2.8g, 4mmol), Potassium acetate (39.3g, 400mmol) and 1,4-dioxane (400ml) were taken in 500 ml round bottom flask and heated at 90˚C under nitrogen. The reaction progress was followed by TLC and after 12h was worked up. The solvent 1,4-dioxane was distilled at 60℃ under vacuum. Then the residue was added into water (500ml) and extracted with MC (3×200ml) and the organic layer was washed with water (2×300ml), dried over anhydrous $MgSO_4$, filtered, and then distilled to dryness under vacuum.

Then the residue was dissolved into hot EA, filtered, and distilled to dryness under vacuum to give crude product. The crude was recrystallized from Hexane to give pure product 33.2g (yield: 90%) as a light-yellow solid. R_f=0.7 (SiO_2, Hex). GC-Mass 369.26, $C_{24}H_{24}BNO_2$, m/z (relative intensity): 369 (100%).

2.2.2.2 Synthesis of compound 2 (5,5'-Di(9-phenylcarbazole-3-yl)-8,8'-biquinoline)

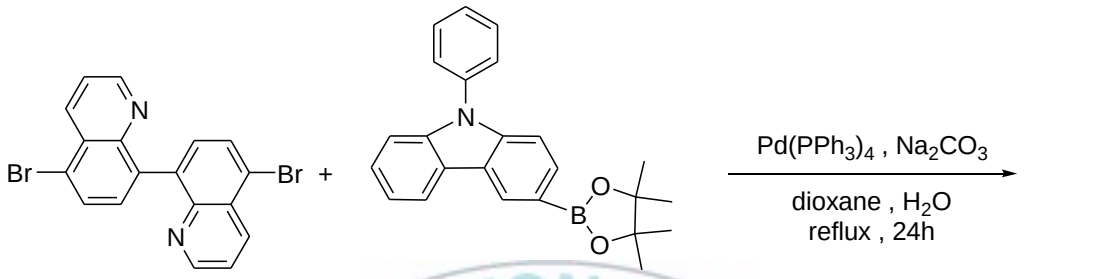

5,5'-dibromo-8,8'-biquinoline

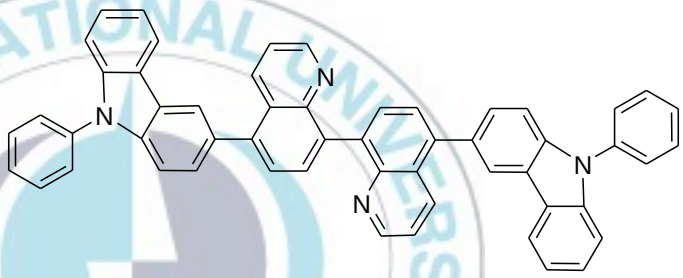

compound 2

5,5'-Dibromo-8,8'-biquinoline (1.2g, 2.9mmol), 2M Na_2CO_3 (8.7ml, 17.4mmol) and 3-(4,4,5,5-Tetramethyl-1,3,2-dioxaborolan-2-yl)-9-phenylcarbazole (3.2g, 8.7mmol) were dissolved in 40ml of dioxane in a dried flask. The solution was purged with nitrogen for 20min, and then tetrakis(triphenylphosphine)palladium (0.2g, 0.174mmol) was added and the reaction mixture was refluxed (85℃) with stirring. The reaction progress was followed by TLC and after 24h was worked up. The cooled mixture was added into water (200ml), filtered and washed with Methanol. The crude product so obtained was purified with silica gel chromatography and eluted with (EA: Hex=1:1) as eluent. Product was recrystallized from THF to give white solid 1.56g (yield: 72.9%, total yield: 9.1%). m.p. 317-318℃, R_f=0.2 (SiO_2, EA: Hex=1:3), ^{1}HNMR (400MHz, $CDCl_3$): δ=8.88 (m, 2H), 8.47 (d, 2H), 8.35 (d, 2H), 8.19 (d, 2H), 7.99 (d, 2H), 7.81 (d, 2H), 7.63-7.67 (m, 10H), 7.57 (d, 2H), 7.50-7.52 (m, 2H), 7.44-7.48 (m, 4H), 7.32-7.36 (m, 4H) ppm. $C_{54}H_{34}N_4$ 738.87.

2.2.3 Synthesis of compound 3 (5,8'-Di(9,9-dimethylfluorene-2-yl)-5',8-biquinoline)

Compound 3 was prepared by using 4,4'-Dibromobiphenyl as start material, via nitrification, reduction, Skraup synthesis, Suzuki coupling reaction.

2.2.3.1 Synthesis of 2,3'-Dinitro-4,4'-dibromobiphenyl

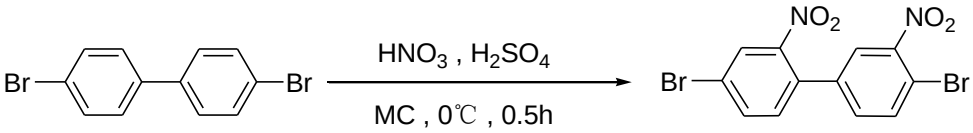

4,4'-dibromobiphenyl — 2,3'-dinitro-4,4'-dibromobiphenyl

A mixture of 99.5% Nitric acid (45ml) and 95% Sulfuric acid (37.5ml) was added dropwise to a solution of 4,4'-Dibromobiphenyl (36g, 115mmol) in MC (144ml) at 0℃ for 0.5 hour. And the reaction mixture was diluted with ice water (600ml), and extracted with MC (3×250ml). The combined organic layers were washed with water (2×450ml), dried over anhydrous $MgSO_4$, and distilled to dryness under vacuum. The crude was recrystallized from EA to give pure product 37g (yield: 80%) as a yellow solid. m.p. 145~146℃, R_f=0.6 (SiO_2, EA: Hex=1:3), ^{1}HNMR (400MHz, $CDCl_3$): δ=8.38 (d, 1H), 8.14 (d, 1H), 8.05-8.08 (dd, 1H), 8.00-8.02 (d, 1H), 7.57-7.62 (m, 2H) ppm. GC-Mass 402.0, $C_{12}H_6Br_2N_2O_4$, m/z (relative intensity): 401 (100%).

2.2.3.2 Synthesis of 4,4'-Dibromobiphenyl-2,3'-diamine

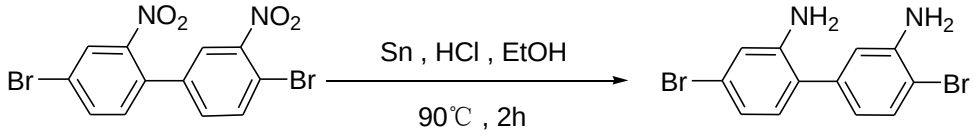

2,3'-dinitro-4,4'-dibromobiphenyl — 4,4'-dibromobiphenyl-2,3'-diamine

To a solution of 2,3'-Dinitro-4,4'-dibromobiphenyl (31.2g, 78mmol) in 370ml of ethanol was added 35% w/w aqueous HCl (221ml). Tin powder (55g, 466mmol) was then added portionwise over 0.5 hour, and the reaction mixture was heated to reflux at 90℃ for 2 hour. After cooling, the mixture was poured into ice water (800ml) and then made alkaline with 30% w/w aqueous NaOH solution until the PH was 9.0. The product was next extracted with MC (3×500ml) and the organic layer was washed with water (5×400ml), dried over anhydrous $MgSO_4$, filtered, and then distilled to dryness under vacuum to give crude product

23g (yield: 86.6%) as a light-brown solid that can be used without further purification. R_f=0.5 (SiO_2, EA: Hex=1:3). GC-Mass 342.03, $C_{12}H_{10}Br_2N_2$, m/z (relative intensity): 342 (100%).

2.2.3.3 Synthesis of 5,8'-Dibromo-5',8-biquinoline

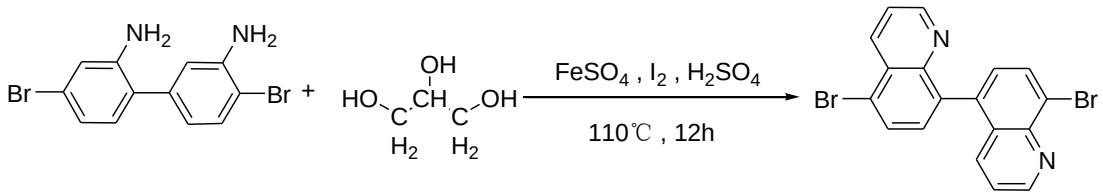

4,4'-dibromobiphenyl-2,3'-diamine glycerol 5,8'-dibromo-5',8-biquinoline

4,4'-Dibromobiphenyl-2,3'-diamine (20.2g, 59mmol), Glycerol (43.6g, 473mmol), Iron(II) sulfate heptahydrate (4.9g, 18mmol), Iodine (0.3g, 1.2mmol), and Sulphuric acid (91ml, 1623mmol) were taken in 500 ml round bottom flask and heated at 110˚C. The reaction progress was followed by TLC and after 12h was worked up. The cooled mixture was neutralized with NaOH and filtered, and the filter cake was dried at 70˚C under vacuum. The crude product so obtained was purified with silica gel chromatography and eluted with (EA: Hex=1:6) as eluent. Product was recrystallized from (THF: Methanol=5:1) to give light-yellow solid 6.8g (yield: 28%). R_f=0.4 (SiO_2, EA: Hex=1:3), ^{1}HNMR (400MHz, $CDCl_3$): δ=9.02 (s, 1H), 8.77 (s, 1H), 8.66 (d, 1H), 8.16 (d, 1H), 7.97 (d, 1H), 7.67 (d, 1H), 7.58 (m, 2H), 7.43 (d, 1H), 7.25 (s, 1H) ppm. GC-Mass 414.09, $C_{18}H_{10}Br_2N_2$, m/z (relative intensity): 413 (100%).

2.2.3.4 Synthesis of compound 3 (5,8'-Di(9,9-dimethylfluorene-2-yl)-5',8-biquinoline)

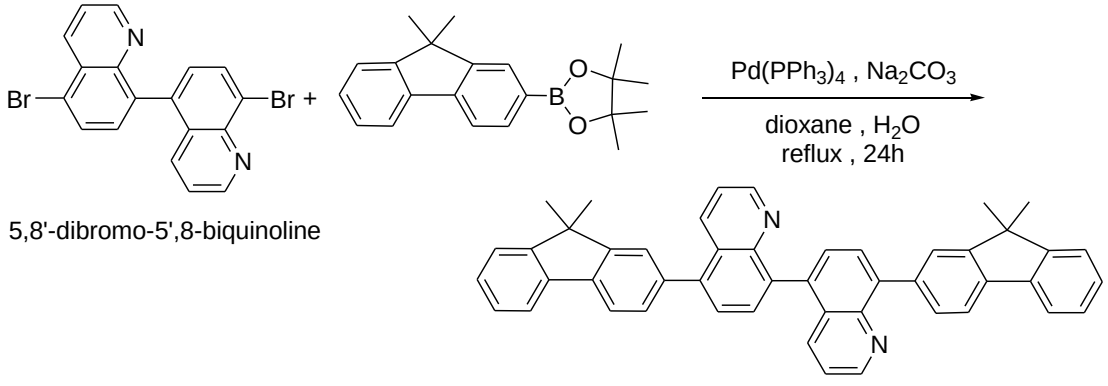

5,8'-dibromo-5',8-biquinoline

compound 3

5,8'-Dibromo-5',8-biquinoline (1.2g, 2.9mmol), 2M Na_2CO_3 (8.7ml, 17.4mmol) and 2-(4,4,5,5-tetramethyl-1,3,2-dioxaborolan-2-yl)-9,9-dimethylfluorene (2.8g, 8.7mmol) were dissolved in 40ml of dioxane in a dried flask. The solution was purged with nitrogen for 20min, and then tetrakis(triphenylphosphine)palladium (0.2g, 0.174mmol) was added and the reaction mixture was refluxed (85℃) with stirring. The reaction progress was followed by TLC and after 24h was worked up. The cooled mixture was added into water (200ml), filtered and washed with Methanol. The crude product so obtained was purified with silica gel chromatography and eluted with (EA: Hex=1:1) as eluent. Product was recrystallized from (THF: Methanol=5:1) to give white solid 1.62g (yield: 87%, total yield: 16.9%). m.p. 313-314℃, R_f=0.25 (SiO_2, EA: Hex=1:3), ^{1}HNMR (400MHz, $CDCl_3$): δ=9.00 (s, 1H), 8.87 (d, 1H), 8.47-8.45 (t, 1H), 7.96-7.87 (m, 4H), 7.86-7.81 (m, 4H), 7.79-7.73 (m, 3H), 7.63 (s, 1H), 7.58-7.54 (m, 1H), 7.51-7.46 (m, 2H), 7.42-7.36 (m, 4H), 7.35-7.31 (m, 1H), 7.29-7.27 (m, 1H), 1.58 (s, 12H) ppm. $C_{48}H_{36}N_2$ 640.81.

2.2.4 Synthesis of compound 4 (5,8'-Di(9-phenylcarbazole-3-yl)-5',8-biquinoline)

Compound 4 was prepared by using 4,4'-Dibromobiphenyl as start material, via nitrification, reduction, Skraup synthesis, Suzuki coupling reaction.

2.2.4.1 Synthesis of compound 4 (5,8'-Di(9-phenylcarbazole-3-yl)-5',8-biquinoline)

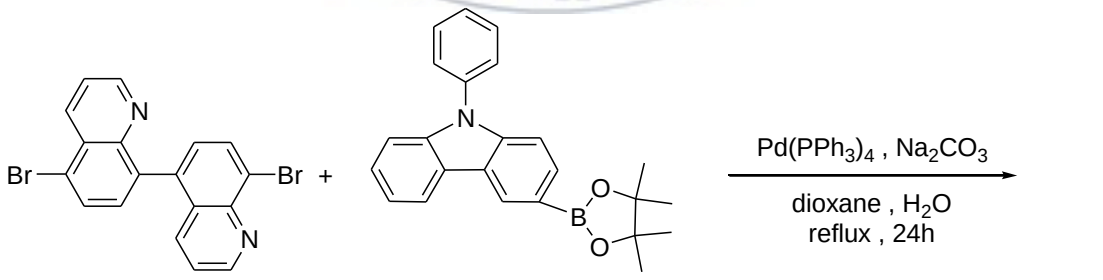

5,8'-dibromo-5',8-biquinoline

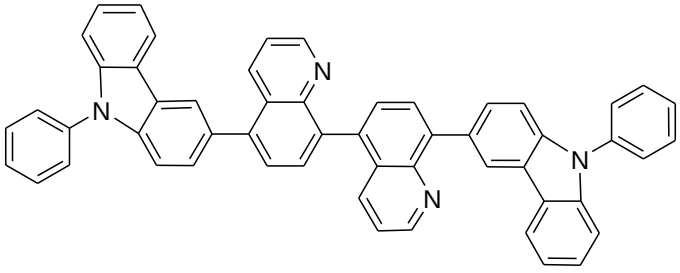

compound 4

5,8'-Dibromo-5',8-biquinoline (1.2g, 2.9mmol), 2M Na_2CO_3 (8.7ml, 17.4mmol) and 3-(4,4,5,5-Tetramethyl-1,3,2-dioxaborolan-2-yl)-9-phenylcarbazole (3.2g, 8.7mmol) were dissolved in 40ml of dioxane in a dried flask. The solution was purged with nitrogen for 20min, and then tetrakis(triphenylphosphine)palladium (0.2g, 0.174mmol) was added and the reaction mixture was refluxed (85℃) with stirring. The reaction progress was followed by TLC and after 24h was worked up. The cooled mixture was added into water (200ml), filtered and washed with Methanol. The crude product so obtained was purified with silica gel chromatography and eluted with (EA: Hex=1:1) as eluent. Product was recrystallized from THF to give white solid 1.71g (yield: 80%, total yield: 15.5%). m.p. 291-292℃, R_f=0.15 (SiO_2, EA: Hex=1:3), ^{1}HNMR (400MHz, $CDCl_3$): δ=9.02 (s, 1H), 8.87 (t, 1H), 8.55 (s, 1H), 8.50 (d, 1H), 8.35 (s, 1H), 8.21-8.19 (t, 2H), 8.03 (d, 1H), 7.99-7.98 (d, 1H), 7.90-7.88 (m, 2H), 7.81-7.79 (t, 2H), 7.68-7.61 (m, 10H), 7.59-7.57 (m, 1H), 7.54-7.51 (m, 1H), 7.49-7.47 (t, 3H), 7.45-7.38 (m, 3H), 7.35-7.32 (m, 1H), 7.31-7.28 (t, 2H) ppm. $C_{54}H_{34}N_4$ 738.87.

2.2.5 Synthesis of compound 5 (6-Phenyl-3,9-di(thiophen-2-yl)-5H-dibenzo[d,f][1,3]diazepine)

Compound 5 was prepared by using 1,4-Dibromobenzene as start material, via nitrification, condensation, reduction, cyclization, Suzuki coupling reaction.

2.2.5.1 Synthesis of 3,9-Dibromo-6-phenyl-5H-dibenzo[d,f][1,3]diazepine

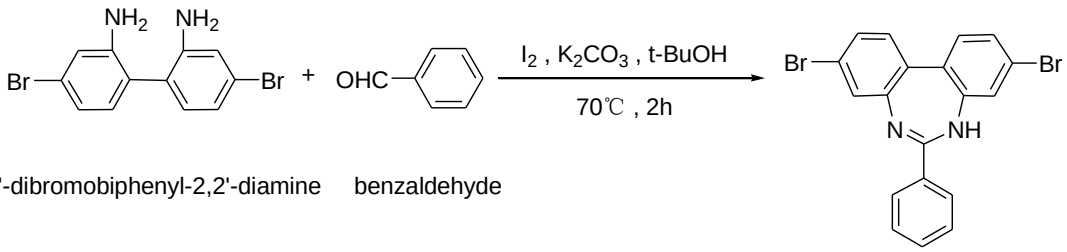

4,4'-dibromobiphenyl-2,2'-diamine benzaldehyde

4,4'-Dibromobiphenyl-2,2'-diamine (15g, 44mmol), Benzaldehyde (4.65g, 44mmol), iodine (33g, 130mmol) and Potassium carbonate (18g, 130mmol) were dissolved in 250mL of t-butylalcohol and heated with stirring at 70˚C. After 2 hour, the reaction mixture was cooled and treated with sodium thiosulfate (1500mL, 5%), filtered and washed with water. Then the filter cake was dried in vacuum oven at 70℃. The crude product so obtained was purified

with silica gel chromatography and eluted with (EA: Hex=1:8) as eluent. The compound was obtained as yellow solid (8g, 42.6%). R_f=0.4 (SiO_2, EA: Hex=1:3), ^{1}HNMR (400MHz, $CDCl_3$): δ=7.87 (d, 2H), 7.52 (t, 1H), 7.50 (t, 2H), 7.40 (bs, 1H), 7.31 (m, 4H), 7.00 (bs, 1H), 6.24 (bs, 1H) ppm. GC-Mass 428.12, $C_{19}H_{12}Br_2N_2$, m/z (relative intensity): 428 (100%).

2.2.5.2 Synthesis of 3,9-Di(4,4,5,5-tetramethyl-1,3,2-dioxaborolan-2-yl)-6-phenyl-5H-dibenzo[d,f][1,3]diazepine

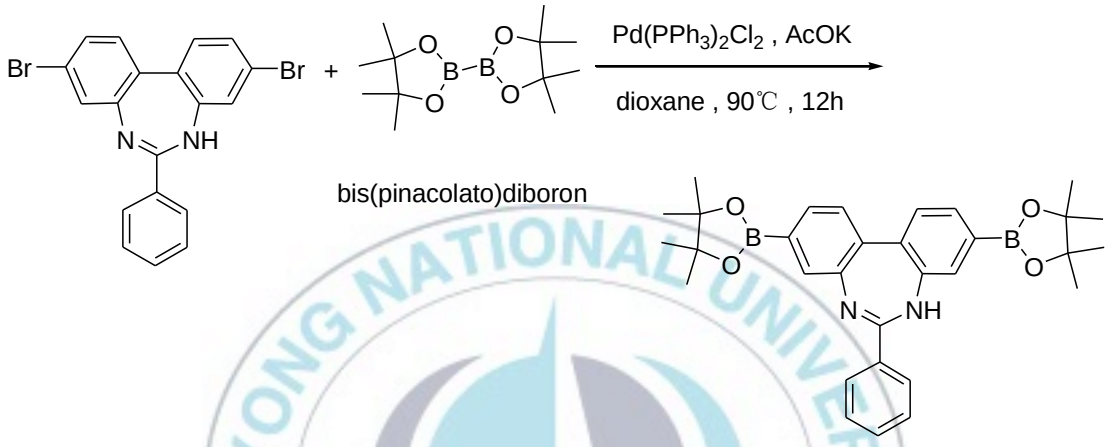

3,9-Dibromo-6-phenyl-5H-dibenzo[d,f][1,3]diazepine (9.7g, 23mmol), Bis(pinacolato)diboron (12.7g, 50mmol), $Pd(PPh_3)_2Cl_2$ (1.27g, 1.81mmol), Potassium acetate (17.8g, 181mmol) and 1,4-dioxane (500ml) were taken in 1000 ml round bottom flask and heated at 90˚C under nitrogen. The reaction progress was followed by TLC and after 12h was worked up. The solvent 1,4-dioxane was distilled at 60℃ under vacuum. Then the residue was added into water (700ml) and extracted with MC (3×300ml) and the organic layer was washed with water (3×400ml), dried over anhydrous $MgSO_4$, filtered, and then distilled to dryness under vacuum. Then the residue was dissolved into hot EA, filtered, and distilled to dryness under vacuum to give crude product. The crude was recrystallized from Hexane to give pure product 10.7g (yield: 90%) as a yellow solid. R_f=0.5 (SiO_2, Hex). GC-Mass 522.25, $C_{31}H_{36}B_2N_2O_4$, m/z (relative intensity): 521 (100%).

2.2.5.3 Synthesis of compound 5

(6-Phenyl-3,9-di(thiophen-2-yl)-5H-dibenzo[d,f][1,3]diazepine)

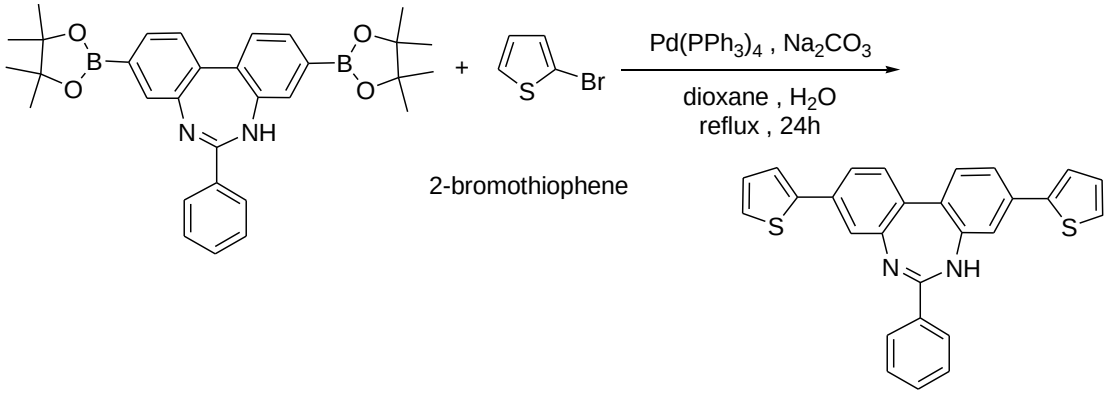

compound 5

3,9-Di(4,4,5,5-tetramethyl-1,3,2-dioxaborolan-2-yl)-6-phenyl-5H-dibenzo[d,f][1,3]diaze pine (4g, 7.7mmol), 2-Bromothiophene (5g, 30.7mmol) and 2M Na_2CO_3 (15.4ml, 30.7mmol) were dissolved in 100ml of dioxane in a dried flask. The solution was purged with nitrogen for 20min, and then tetrakis(triphenylphosphine)palladium (0.36g, 0.31mmol) was added and the reaction mixture was refluxed (85℃) with stirring. The reaction progress was followed by TLC and after 24h was worked up. The reaction mixture was cooled, extracted with MC (3×300ml), and the extract was washed with saturated brine (3×400ml) and dried over $MgSO_4$. The crude product so obtained was purified with silica gel chromatography and eluted with (EA: Hex=1:18) as eluent. The product was obtained as yellow solid (0.9g, 27%, total yield: 5.1%). m.p. 230-231℃, R_f=0.3 (SiO_2, EA: Hex=1:3), ^{1}HNMR (400MHz, $CDCl_3$): δ=7.87 (bs, 2H), 7.47-7.45 (m, 2H), 7.42-7.38 (m, 3H), 7.36-7.32 (m, 6H), 7.26 (bs, 2H), 7.04 (bs, 2H) ppm. GC-Mass 434.58, $C_{27}H_{18}N_2S_2$, m/z (relative intensity): 434 (100%).

2.2.6 Synthesis of compound 6

(6-Phenyl-3,9-di(furan-2-yl)-5H-dibenzo[d,f][1,3]diazepine)

Compound 6 was prepared by using 1,4-Dibromobenzene as start material, via nitrification, condensation, reduction, cyclization, Suzuki coupling reaction.

2.2.6.1 Synthesis of 2-Bromofuran

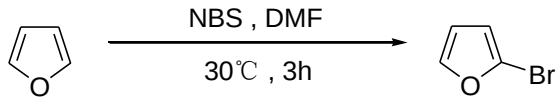

furan 2-bromofuran

A solution of NBS (20g, 0.112mol) in DMF (60ml) was added via addition funnel to a solution of furan (15.3g, 0.225mol) in DMF (40ml) in a 500ml round-bottom flask over a period of 1h, keeping temperature between 25-35℃ under constant stirring. Addition of NBS solution to reaction mixture was found to be exothermic. During addition, the reaction mixture went from brown solution to dark green. After the addition was complete, the reaction mixture was stirred at ambient temperature for an additional 3h. The resulting clear brown solution was heated gradually to 100-110℃ to distill out some of the unreacted furan. After maintaining 100-110℃ temperature for 0.5-1h, the reaction mixture was exposed to a constant jet of steam generated by heating distilled water to 100-120℃ in a separate round-bottom flask. Distillate consisting of water and 2-Bromofuran was collected in a receiver. The initial few drops contained mostly residual unreacted furan and were therefore collected separately. Distillation continued until no organic product was present in the distillate. The distillate was transferred to a separatory funnel along with water (20-30ml). The suspension was shaken well to force traces of DMF to the aqueous layer. After layer separation, the 2-Bromofuran settled down as a colorless lower layer, which was collected and stored in a dry bottle containing anhydrous K_2CO_3 (7.2g, 44%). ^{1}HNMR (400MHz, $CDCl_3$): δ=6.28 (dd, 1H), 6.35 (dd, 1H), 7.40 (dd, 1H) ppm. GC-Mass 146.97, C_4H_3BrO, m/z (relative intensity): 146 (100%).

2.2.6.2 Synthesis of compound 6

(6-Phenyl-3,9-di(furan-2-yl)-5H-dibenzo[d,f][1,3]diazepine)

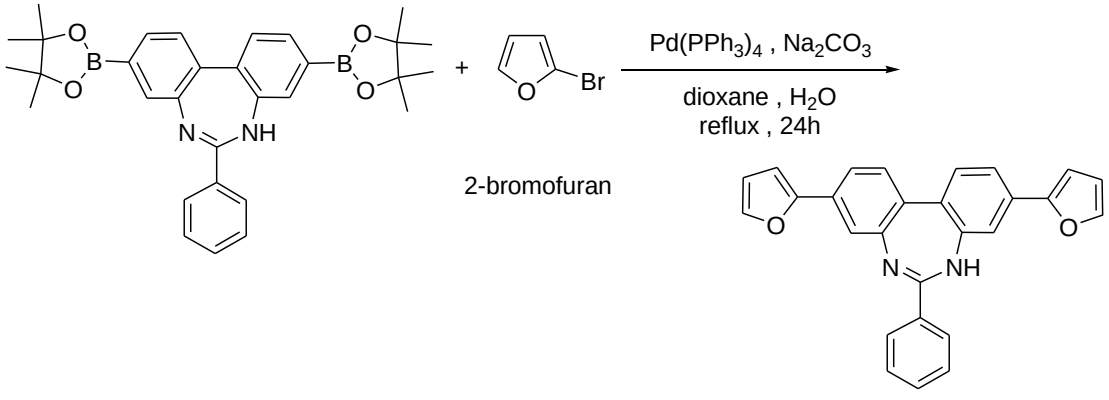

compound 6

3,9-Di(4,4,5,5-tetramethyl-1,3,2-dioxaborolan-2-yl)-6-phenyl-5H-dibenzo[d,f][1,3]diazepine (4g, 7.7mmol), 2-Bromofuran (4.5g, 30.7mmol) and 2M Na_2CO_3 (15.4ml, 30.7mmol) were dissolved in 100ml of dioxane in a dried flask. The solution was purged with nitrogen for 20min, and then tetrakis(triphenylphosphine)palladium (0.36g, 0.31mmol) was added and the reaction mixture was refluxed (85℃) with stirring. The reaction progress was followed by TLC and after 24h was worked up. The reaction mixture was cooled, extracted with MC (3×300ml), and the extract was washed with saturated brine (3×400ml) and dried over $MgSO_4$. The crude product so obtained was purified with silica gel chromatography and eluted with (EA: Hex=1:18) as eluent. The product was obtained as yellow solid (0.86g, 28%, total yield: 5.2%). m.p. 225-226℃, R_f=0.3 (SiO_2, EA: Hex=1:3), ^{1}HNMR (400MHz, $CDCl_3$): δ=7.95 (d, 2H), 7.55-7.45 (m, 6H), 7.42 (m, 4H), 6.70 (d, 2H), 6.50 (m, 2H), 6.34 (bs, 1H) ppm. GC-Mass 402.44, $C_{27}H_{18}N_2O_2$, m/z (relative intensity): 402 (100%).

2.3 Analysis

2.3.1 ^{1}HNMR spectrum

The sample was dissolved in purified $CDCl_3$, and filtered through a 0.45μm filter paper, then measured by 400MHz ^{1}H Nuclear Magnetic Resonance Spectrometer (JNM ECP-400 JEOL社 (Japan)). We can confirm the sample's structure by the protons of benzene rings and alkyl groups corresponding to the peak area ratio. ^{1}HNMR results are included in the Appendix.

2.3.2 DSC (Differential Scanning Calorimetry)

The measurement was performed on a DSC 60 (SHIMATSU Co., Ltd). The sample 3mg was placed in the Aluminium PAN, compressed by the compressor and then at a heating rate of 10℃/min under a nitrogen gas flow.

2.3.3 Evaluation of the optical properties

UV-Vis absorption spectrum and photoluminescence spectrum were measured by UV-Vis spectrophotometer (M-3150, SHIMADZU Co., Ltd) and Fluorescence spectrophotometer (F-450 HITACHI Co., Ltd), respectively. The sample 1mg was dissolved in purified Tetrahydrofuran 5ml to prepare a solution and then measured the absorbance and luminescence properties.

2.3.4 Cyclic Voltammetry

The sample's Cyclic voltammogram was measured by WPG-200 (WonA-tech Co., Ltd). Pt wire was regarded as a working electrode, Ag/AgCl (in 3M NaCl) was regarded as a reference electrode, Au wire was regarded as an auxiliary electrode, measured at the scan rate of 100mV/s. Tetrabutylammonium hexafluorophosphate (98%) was dissolved in purified ACN, and prepared 0.1M solution, then used as an electrolyte. In addition, 0.001M Ferrocene was used to correct Ag/AgCl potential.

3. Results and Discussions

3.1 Synthesis of organic electron-transport materials

In this research, biquinoline and diazepine were used as the precursors of organic electron-transport in order to obtain excellent characteristics, such as appropriate HOMO, LUMO and Band gap value, high thermal stability and oxidative stability.

Compound 1~4 were synthesized from the corresponding diamino compounds. The diamino compounds were ring closed to the corresponding biquinoline molecules via Skraup synthesis using Glycerol in the presence of Sulfuric acid and Iodine. Then the biquinoline compounds were coupled with N-phenylcarbazole and 9,9-dimethylfluorene via Suzuki synthesis using the catalyst Tetrakis(triphenylphosphine)palladium(0)($Pd(PPh_3)_4$) in the presence of Sodium carbonate(Na_2CO_3), 1,4-dioxane and water.

Compound 5~6 were synthesized from 2,2'-Diamino-4,4'-dibromobiphenyl. The diamino compound was converted to diazepine compound by a simple and fast one-step reaction with Benzaldehyde in the presence of Potassium carbonate and Iodine using t-Butanol as the solvent. Then the diazepine compound was coupled with thiophen and furan compounds via Suzuki synthesis using the catalyst Tetrakis(triphenylphosphine)palladium(0)($Pd(PPh_3)_4$) in the presence of Sodium carbonate(Na_2CO_3), 1,4-dioxane and water.

3.2 Spectral characteristics of compounds

In order to obtain the optical properties of the compound, a sample solution in THF was measured to give the UV-Vis absorption spectrum and photoluminescence spectrum. From the beginning of the absorption spectrum curve, the compound can be seen a sharp change in light absorption. After the compound absorbs light energy from the outside, the internal electrons jump from the ground state to an excited state. The energy charge absorbed is determined by the polaron's energy gap. If the compound has a asymmetric structure, then it has π orbital and π* orbital two forms. Each band π orbital and π* orbital generated does not overlap each other. Because of certain difference in Band gap, Band to band transition occurs. Fluorescence spectrum was measured at the maximum absorption wavelength of the compound. Cut off wavelength and Band gap can be obtained through absorption spectrum and photoluminescence spectrum.

3.2.1 Spectral characteristics of Compound 1

Figure. 12 is the measuring result of UV-Vis. absorption and PL spectrum. The data of spectral characteristics refer to Table 1. In the UV-Vis. absorption spectrum, the maximum absorption wavelength (Abs λ_{max}) is at 325nm (π-π* transition). Exciting at the maximum absorption wavelength, the maximum photoluminescence peak is seen at 421.2nm. According to the data of UV and PL spectrum, we can calculate Cut off wavelength is at 370nm and Band gap is 3.35eV.

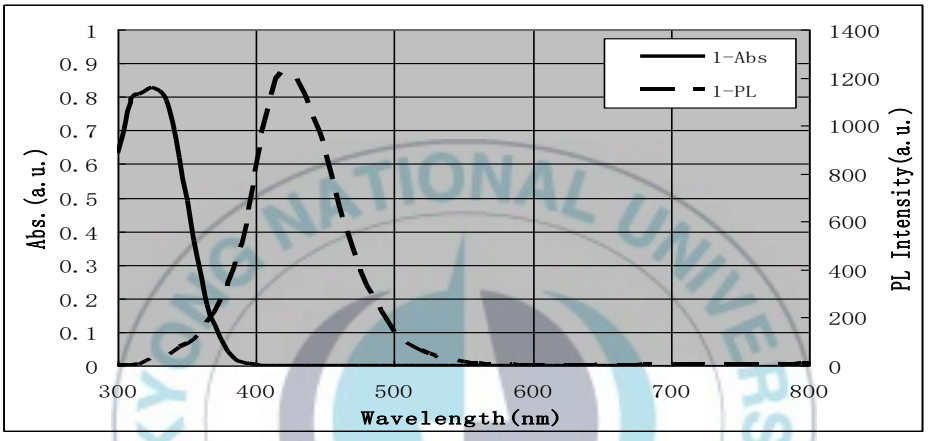

Figure 12. UV-Vis. absorption and photoluminescence spectra of Compound 1 in the THF solution

Table 1. Spectral characteristics of Compound 1 in the THF solution

Sample Name		Compound 1
Solution	Abs. λ_{max} (nm)	325
	PL λ_{max} (nm)	421.2
	Stoke's shift (nm)	96.2
	Cut off wavelength (nm)	370
	Band gap (eV)	3.35

3.2.2 Spectral characteristics of Compound 2

Figure. 13 is the measuring result of UV-Vis. absorption and PL spectrum. The data of spectral characteristics refer to Table 2. In the UV-Vis. absorption spectrum, the maximum absorption wavelength (Abs λ_{max}) is at 334nm (π-π* transition). Exciting at the maximum absorption wavelength, the maximum photoluminescence peak is seen at 431.2nm. According to the data of UV and PL spectrum, we can calculate Cut off wavelength is at 375nm and Band gap is 3.31eV.

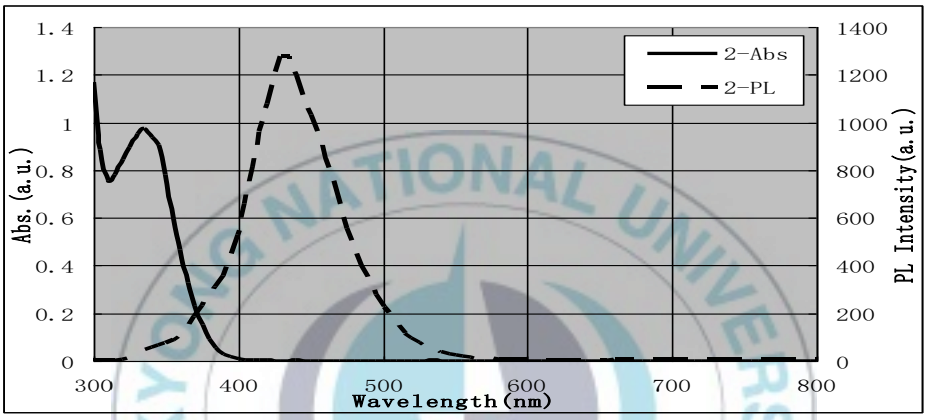

Figure 13. UV-Vis. absorption and photoluminescence spectra of Compound 2 in the THF solution

Table 2. Spectral characteristics of Compound 2 in the THF solution

Sample Name		Compound 2
Solution	Abs. λ_{max} (nm)	334
	PL λ_{max} (nm)	431.2
	Stoke's shift (nm)	97.2
	Cut off wavelength (nm)	375
	Band gap (eV)	3.31

3.2.3 Spectral characteristics of Compound 3

Figure. 14 is the measuring result of UV-Vis. absorption and PL spectrum. The data of spectral characteristics refer to Table 3. In the UV-Vis. absorption spectrum, the maximum absorption wavelength (Abs λ_{max}) is at 335nm (π-π* transition). Exciting at the maximum absorption wavelength, the maximum photoluminescence peak is seen at 431.4nm. According to the data of UV and PL spectrum, we can calculate Cut off wavelength is at 370nm and Band gap is 3.35eV.

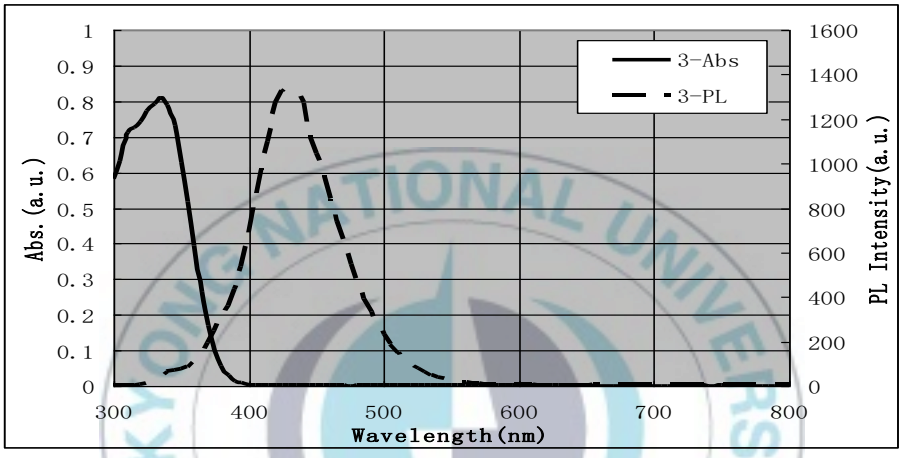

Figure 14. UV-Vis. absorption and photoluminescence spectra of Compound 3 in the THF solution

Table 3. Spectral characteristics of Compound 3 in the THF solution

Sample Name		Compound 3
Solution	Abs. λ_{max} (nm)	335
	PL λ_{max} (nm)	431.4
	Stoke's shift (nm)	96.4
	Cut off wavelength (nm)	370
	Band gap (eV)	3.35

3.2.4 Spectral characteristics of Compound 4

Figure. 15 is the measuring result of UV-Vis. absorption and PL spectrum. The data of spectral characteristics refer to Table 4. In the UV-Vis. absorption spectrum, the maximum absorption wavelength (Abs λ_{max}) is at 345nm (π-π* transition). Exciting at the maximum absorption wavelength, the maximum photoluminescence peak is seen at 444.0nm. According to the data of UV and PL spectrum, we can calculate Cut off wavelength is at 380nm and Band gap is 3.26eV.

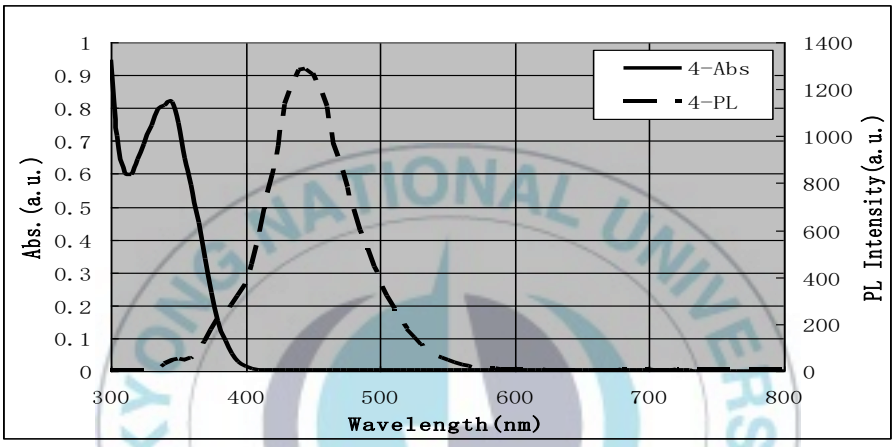

Figure 15. UV-Vis. absorption and photoluminescence spectra of Compound 4 in the THF solution

Table 4. Spectral characteristics of Compound 4 in the THF solution

Sample Name		Compound 4
Solution	Abs. λ_{max} (nm)	345
	PL λ_{max} (nm)	444.0
	Stoke's shift (nm)	99.0
	Cut off wavelength (nm)	380
	Band gap (eV)	3.26

3.2.5 Spectral characteristics of Compound 5

Figure. 16 is the measuring result of UV-Vis. absorption and PL spectrum. The data of spectral characteristics refer to Table 5. In the UV-Vis. absorption spectrum, the maximum absorption wavelength (Abs λ_{max}) is at 320nm (π-π* transition). Exciting at the maximum absorption wavelength, the maximum photoluminescence peak is seen at 415.2nm. According to the data of UV and PL spectrum, we can calculate Cut off wavelength is at 381nm and Band gap is 3.25eV.

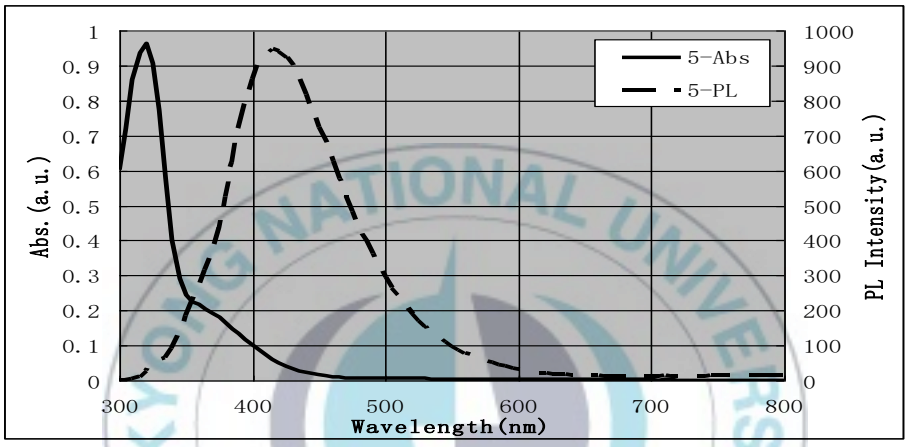

Figure 16. UV-Vis. absorption and photoluminescence spectra of Compound 5 in the THF solution

Table 5. Spectral characteristics of Compound 5 in the THF solution

Sample Name		Compound 5
Solution	Abs. λ_{max} (nm)	320
	PL λ_{max} (nm)	415.2
	Stoke's shift (nm)	95.2
	Cut off wavelength (nm)	381
	Band gap (eV)	3.25

3.2.6 Spectral characteristics of Compound 6

Figure. 17 is the measuring result of UV-Vis. absorption and PL spectrum. The data of spectral characteristics refer to Table 6. In the UV-Vis. absorption spectrum, the maximum absorption wavelength (Abs λ_{max}) is at 319nm (π-π* transition). Exciting at the maximum absorption wavelength, the maximum photoluminescence peak is seen at 413.8nm. According to the data of UV and PL spectrum, we can calculate Cut off wavelength is at 380nm and Band gap is 3.26eV.

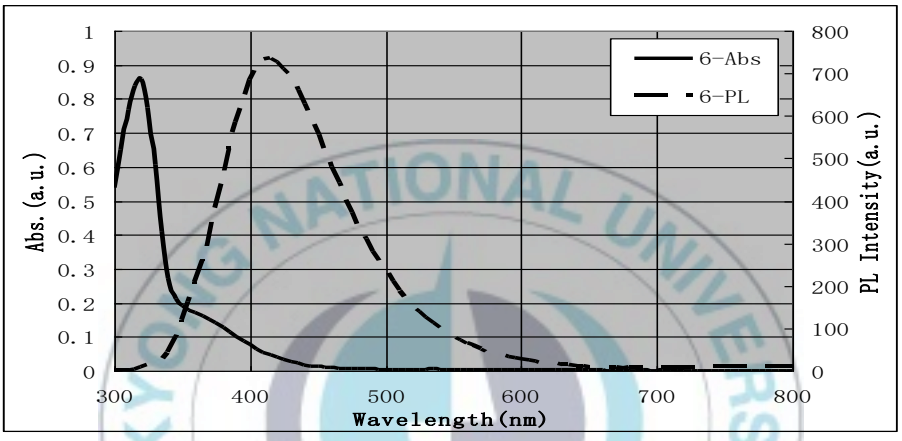

Figure 17. UV-Vis. absorption and photoluminescence spectra of Compound 6 in the THF solution

Table 6. Spectral characteristics of Compound 6 in the THF solution

Sample Name		Compound 6
Solution	Abs. λ_{max} (nm)	319
	PL λ_{max} (nm)	413.8
	Stoke's shift (nm)	94.8
	Cut off wavelength (nm)	380
	Band gap (eV)	3.26

3.3 Thermal characteristics of compounds

Figure. 18~21 and Table 7 is the measuring result of organic ompounds' DSC. In the four compounds synthesized by biquinoline and its isomers as precursors, Compound 1 has the highest thermal stability. In addition, between the two compounds synthesized by diazepine as precursor, Compound 5 has the highest thermal stability. From the curves, we can learn six compounds all haven't glass transition process, so they haven't glass transition temperature (T_g).

Table 7. Thermal characteristics of organic compounds

Sample Name	Melting Point (T_m, ℃)
Compound 1	336.6
Compound 2	318.1
Compound 3	313.6
Compound 4	291.9
Compound 5	230.9
Compound 6	225.3

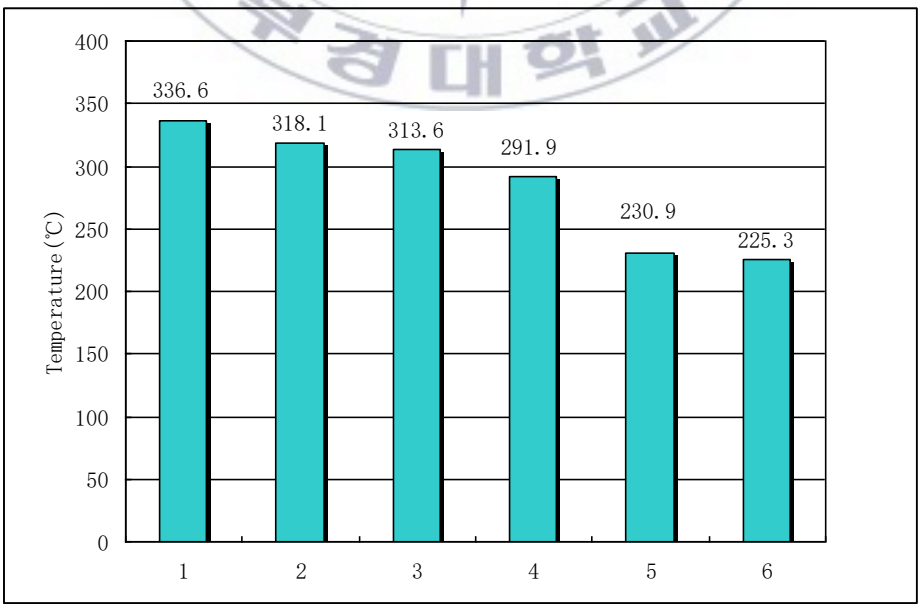

Figure 18. Comparison of compounds by melting point

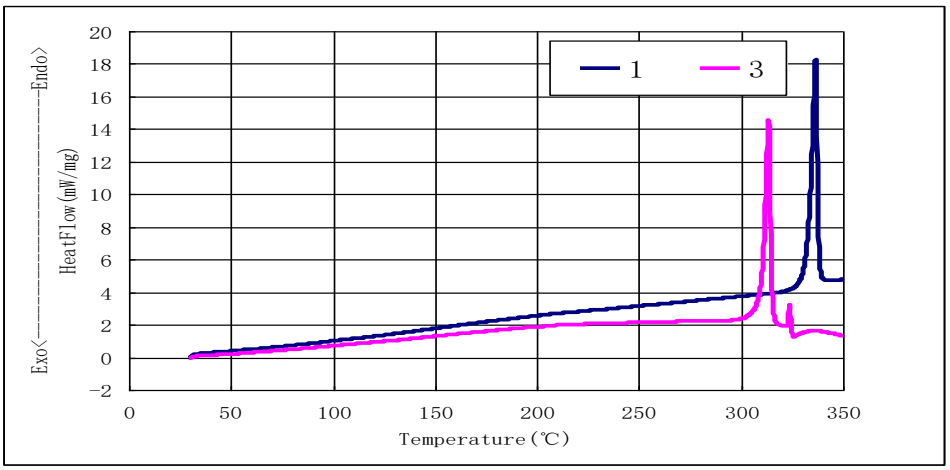

Figure 19. DSC Curves of Compound 1, 3

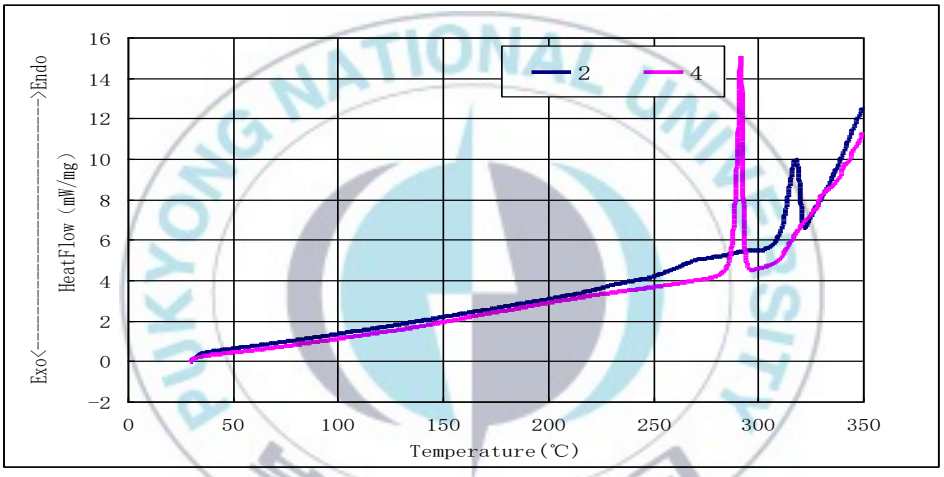

Figure 20. DSC Curves of Compound 2, 4

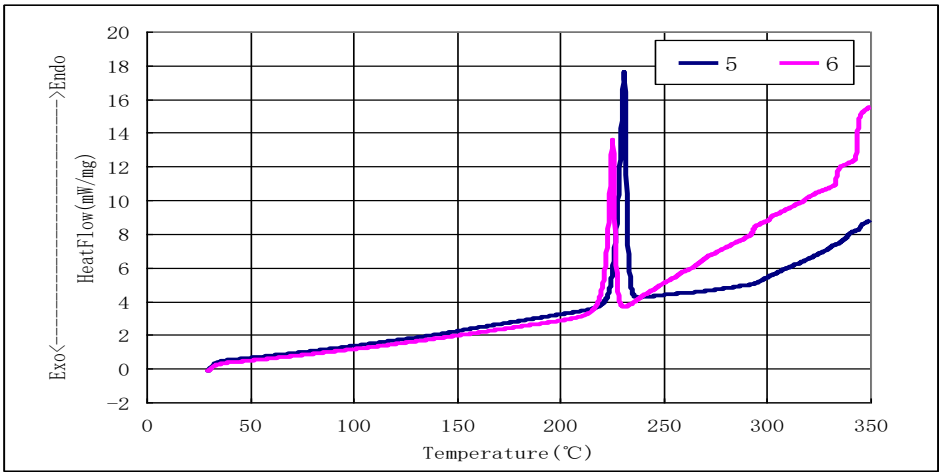

Figure 21. DSC Curves of Compound 5, 6

3.4 Electrical characteristics of compounds

3.4.1 Cyclic Voltammetry (CV)

Cyclic Voltammetry is one of the most important electrochemical analysis methods. CV explains the oxidation-reduction characteristics of the compound, studies the reaction process of the oxidation-reduction and the electrode reaction rate. The current can be obtained within a certain range by changing the voltage. When the voltage begins to increase from the point, the amount of increasing current can be expected. However, when the current increases greater than the diffusion rate of the solute in the potential range, diffusion process is blocked, current does not increase with increasing potential. Instead, the diffusion layer around the electrode is increased, concentration gradient becomes smaller, current value decreases again after reaching its peak.

Measured by Cyclic Voltammetry, in figure 22 (A), within the error range 0.1eV, with the place to start oxidation $[E_{onset}]^{OX}$ value, HOMO value was calculated. 0.001M Ferrocene was used to correct Ag/AgCl potential. Its HOMO value was 4.82eV that the reference electrode Ag/AgCl had a relatively stable value in the ACN solution. Namely, the value measured by Cyclic Voltammetry plus 4.82eV equal the HOMO value. This indicates by the formula (1). In figure 22 (B), Band gap value can be calculated by using Cut off wavelength value of UV-Vis absorption. Then LUMO value can be calculated by HOMO value plus Band gap value.

Figure 23. is the Cyclic Voltammograms of compounds. HOMO, LUMO, Band gap values shown in Table 8. can be calculated by following three formulas (1), (2), (3).

$$E_{HOMO} = -\,([E_{onset}]^{OX} + 4.82)\ eV \quad \cdots\cdots\cdots\cdots (1)$$

$$\text{Band gap energy } (E_g) = hc / \lambda \quad \cdots\cdots\cdots\cdots\cdots (2)$$

$$E_{LUMO} = E_{HOMO} + E_g \quad \cdots\cdots\cdots\cdots\cdots\cdots\cdots (3)$$

(E_{onset} = onset potentials of the first oxidation wave determined by Cyclic Voltammetry,

h = Planks constant = 6.626×10^{-34} J s,

c =Speed of light = 3.0×10^{8} m/s,

λ =Cut off wavelength (nm))

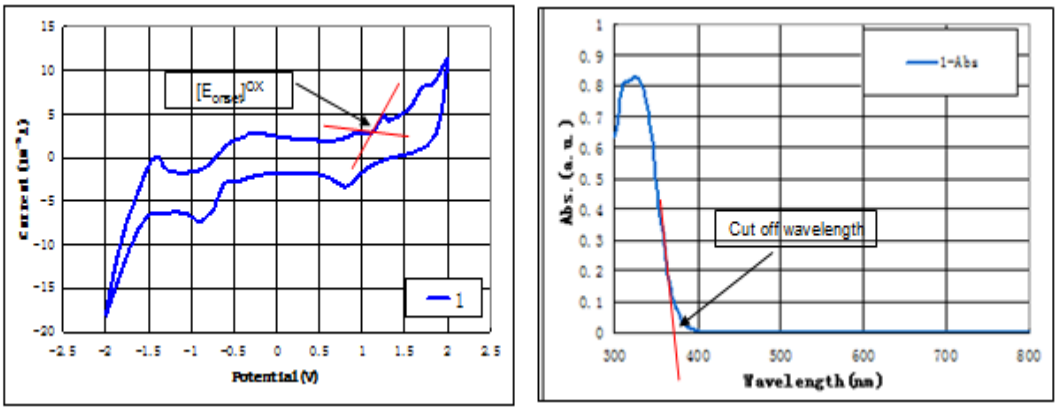

A B

Figure 22. Cyclic Voltammogram and UV-Vis. absorption spectra

Table 8. Electrochemical potentials and energy levels of organic compounds

Sample Name	E_{onset} (eV)	HOMO (eV)	LUMO (eV)	E_g (eV)
Compound 1	1.341	-6.161	-2.811	3.35
Compound 2	1.243	--6.063	-2.753	3.31
Compound 3	1.290	--6.110	-2.760	3.35
Compound 4	0.634	-5.454	-2.194	3.26
Compound 5	1.240	-6.060	-2.810	3.25
Compound 6	1.230	-6.050	-2.790	3.26

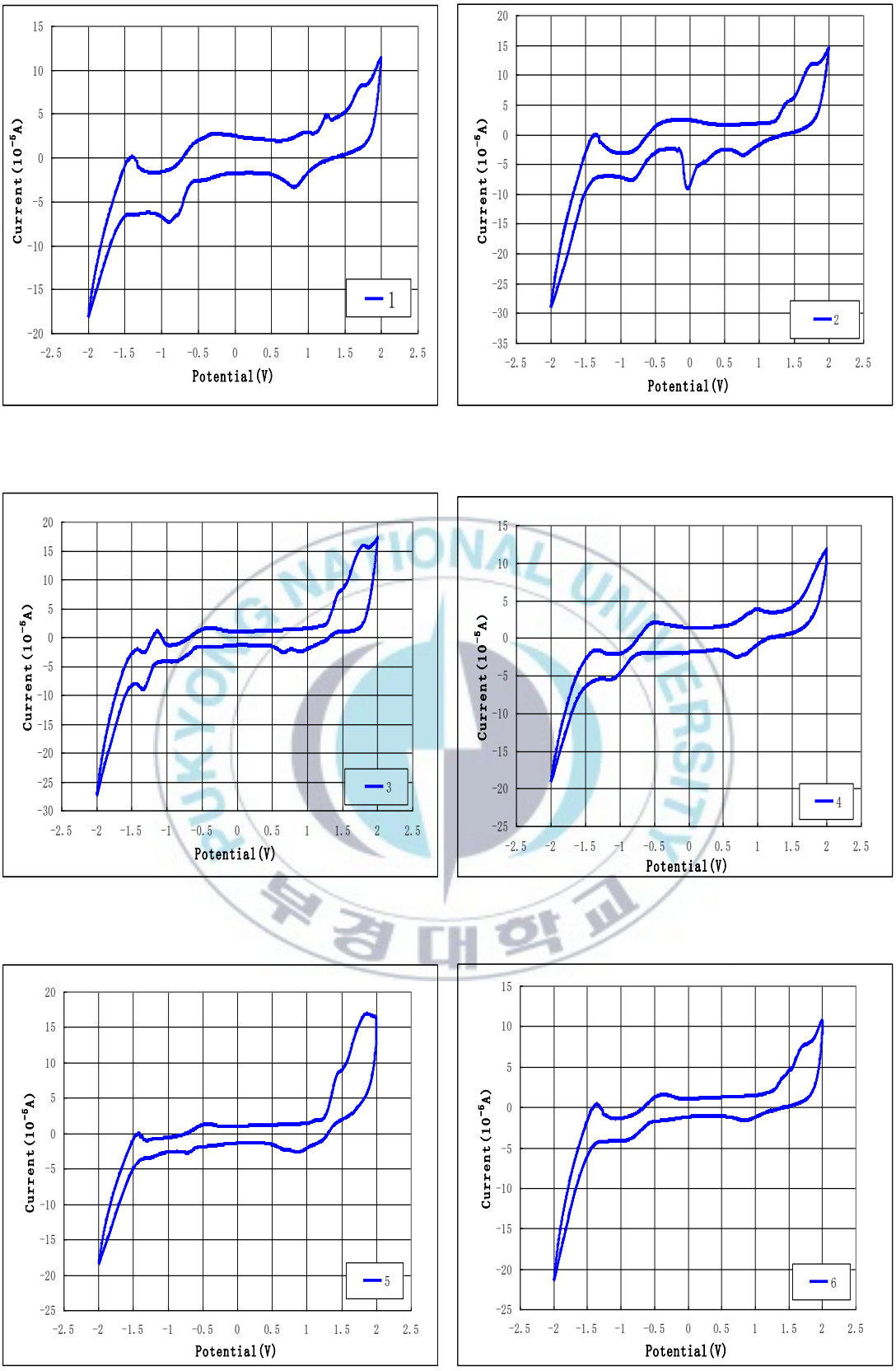

Figure 23. Cyclic Voltammograms of organic compounds

4. Conclusions

In this paper, biquinoline and its isomers as precursors, 9,9-dimethylfluorene and N-phenylcarbazole as substituent groups, four compounds were synthesized. In addition, diazepine as precursor, thiophene and furan as substituent groups, two compounds were synthesized.

This synthesis route is simple and fast, meanwhile has a high yield. Its synthesis process is easier than former methods, because it has only two main steps. In addition, the after-treatment of reaction is easy and convenient. Through a lot of experiments, the best conditions of cyclization reaction and Suzuki coupling reaction were determined. This synthesis route can be used for large scale production of quinoline and diazepine derivatives electron-transport material.

From the results we can learn the thermal stability of quinoline derivatives with a symmetrical structure is better than their isomers with an asymmetric structure. Such as Compound 1 (336.6℃) ＞Compound 3 (313.6℃), Compound 2 (318.1℃) ＞Compound 4 (291.9℃). Due to the molecules with a symmetrical structure can form a better crystallization, therefore it has better thermal stability. Furthermore, the thermal stability of quinoline derivatives with a 9,9-dimethylfluorenyl group is better than the derivatives include a N-phenylcarbazolyl group. Such as Compound 1 (336.6℃) ＞Compound 2 (318.1℃), Compound 3 (313.6℃) ＞ Compound 4 (291.9℃). Due to the molecules with a 9,9-dimethylfluorenyl group have a better plane structure and higher conjugation, therefore they can not only close-packed, but also enhance the dipole interaction between them. Between two diazepine derivatives, Compound 5 (230.9℃) has a thiophene group has better thermal stability than Compound 6 (225.3℃) contains a furan group.

HOMO values of six compounds are all low, so these compounds are not easily oxidized in air and have high oxidative stability. These compounds will have a long lifetime when they are used in devices. And Compound 1 has the lowest HOMO value (-6.161eV), so it has the highest oxidative stability.

Compound 1 has the lowest LUMO value, so it lightly gets electrons and this is helpful

to inject electrons. Furthermore, it has the lowest HOMO value, so it has the ability of blocking holes, too. Its HOMO (-6.161eV) an LUMO (-2.811eV) are lower than PBD (HOMO=-6.06eV, LUMO=-2.16eV), so it has a better electron-transport ability than PBD.

Between two diazepine derivatives, Compound 5 has lower HOMO and LUMO value, so it is better.

From the above measurement results of six compounds, including to UV-Vis, PL, DSC and CV, we can calculate out many important data, including to E_g, HOMO and LUMO. At the same time, we can predict the more suitable compound for using in OLED electron-transport layer by these data.

In this research, the electric characteristics, oxidative stability and thermal stability of compounds can be controlled by varying the functional groups. From these data, we can draw a conclusion that Compound 1 is the most suitable electron-transport material, because it has the lowest HOMO and LUMO value, the maximum Band gap (E_g) value and the highest oxidative stability and thermal stability.

5. References

[1] Klauk, H. *Chem. Soc. Rev.* **2010**, 39, 2643-2666.

[2] Grimsdale, A. C.; Leok Chan, K.; Martin, R. E.; Jokisz, P. G.; Holmes, A. B. *Chem. Rev.* **2009**, 109, 897-1091.

[3] Sakuratani, Y.; Watanabe, T.; Miyata, S. *Thin Solid Films.* **2001**, 388, 256-259.

[4] Itoh, E.; Yamashita, T.; Miyairi, K. *Thin Solid Films.* **2001**, 393, 368-373.

[5] Kido, J.; Iizumi, Y. *Appl. Phys. Lett.* **1998**, 73, 2721.

[6] Kido, J.; Shionoya, H.; Nagai, K. *Appl. Phys. Lett.* **1995**, 67, 2281.

[7] Pope, M.; Kallmann, H. P.; Magnante, P. *J. Chem. Phys.* **1963**, 38, 2042.

[8] Vincett, P. S.; Barlow, W. A.; Hann, R. A.; Roberts, G. G. *Thin Solid Films.* **1982**, 94, 171.

[9] Tang, C. W.; VanSlyke, S. A.; *Appl. Phys. Lett.* **1987**, 51, 913-915.

[10] Burroughes, J. H.; Bradley, D. D. C.; Brown, A. R.; Marks, R. N.; Mackay, K.; Friend, R. H.; Burns, P. L.; Holmes, A. B. *Nature*. **1990**, 347, 539-541.

[11] Braun, D.; Heeger, A. J. *Thin Solid Films*. **1992**, 216, 96-98.

[12] Baldo, M. A.; O'Brien, D. F.; You, Y.; Shoustikov, A.; Sibley, S.; Thompson, M. E.; Forrest, S. R. *Nature.* **1998**, 395, 151.

[13] Adachi, C.; Tokito, S.; Tsutsui, T.; Saito, S. Japan. *J. Appl. Phys.* Part 2, **1988**, 27, L713.

[14] Era, M.; Adachi, C.; Tsutsui, T.; Saito, S. *Chem. Phys. Lett.* **1991**, 178, 488.

[15] Kido, J.; Kohda, M.; Okuyama, K.; Nagai, K. *Appl. Phys. Lett.* **1992**, 61, 761.

[16] Friend, R. H.; Gymer, R. W.; Holmes, A. B. et al. *Nature.* **1999**, 397, 121-128.

[17] Halls, J. J. M.; Baigent, D. R.; Cacialli, F. et al. *Thin Solid Films.* **1996**, 276, 13-20.

[18] Lee, C. L.; Lee, K. B.; Kim. J. J. et al. *Appl. Phys. Lett.* **2000**, 77, 2280-2283.

[19] Lee, J. H.; Liao, C. C.; Hu, P. J.; Chang, Y. *Synth. Met.* **2004**, 144, 279.

[20] Chen, C. H.; Tang, C. W.; Shi, J.; Klubek, K. P. *Macromol. Symp.* **1997**, 125, 49.

[21] Wakimoto, T.; Yonemoto, Y.; Funaki, J.; Tsuchida, M.; Murayama, R.; Nakada, H.; Matsumoto, H.; Yamamura, S.; Nomura, M. *Synth. Met.* **1997**, 91, 15.

[22] Culligan, S. W.; Chen, A. C.; Wallace, J. U.; Klubek, K. P.; Tang, C. W.; Chen, S. H. *Adv. Funct. Mater.* **2006**, 16, 1481.

[23] Shah, B. K.; Neckers, D. C.; Shi, J.; Forsythe, E. W.; Morton, D. *Chem. Mater.* **2006**, 18, 603.

[24] Kim, Y. H.; Shin, D. C.; Kim, S. H. et al. *Adv. Mater.* **2001**, 13, 1690.

[25] Vanslyke, S. A.; Chen, C. H.; Tang, C. W. *Appl. Phys. Lett.* **1996**, 69, 2160.

[26] Anthopoulos, T. D.; Markham, J. P. J.; Namdas, E. B. et al. *Appl. Phys. Lett.* **2003**, 82, 4828.

[27] Adamovich, V. I.; Cordero, S. R.; Djurovich, P. I. et al. *Org. Electron.* **2003**, 4, 77.

[28] Zhang, X.; Shetty, A. S.; Jenekhe, S. A. *Acta Polym.* **1998**, 49, 52-55.

[29] Kim, J. L.; Kim, J. K.; Cho, H. N.; Kim, D. Y.; Kim, C. Y.; Hong, S. I. *Macromolecules.* **2000**, 33, 5880-5885.

[30] Chiang, C. L.; Shu, C. F. *Chem. Mater.* **2002**, 14, 682-687.

[31] Simas, E. R.; Martins, T. D.; Atvars, T. D. Z.; Akcelrud, L. *J. Lumin.* **2009**, 129, 119-125.

[32] Zhan, X.; Liu, Y.; Wu, X.; Wang, S.; Zhu, D. *Macromolecules.* **2002**, 35, 2529-2537.

[33] Kanbara, T.; Yamamoto, T. *Chem. Lett.* **1993**, 419-422.

[34] Liu, S. P.; Ng, S. C.; Chan, H. S. O. *Synth. Met.* **2005**, 149, 1-11.

[35] Li, J.; Grimsdale, A. C. *Chem. Soc. Rev.* **2010**, 39, 2399-2410.

[36] Zhu, H.; Tong, H.; Gong, Y.; Shao, S.; Deng, C.; Yuan, W. Z.; Zhang, Y. J. *Polym. Sci., Part A: Polym. Chem.* **2012**, 50, 2172-2181.

[37] Subbiah, J.; Amb, C. M.; Irfan, I.; Gao, Y.; Reynolds, J. R.; So, F. *ACS Appl. Mater. Interface.* **2012**, 4, 866-870.

[38] Kim, J.; Yun, M. H.; Anant, P.; Cho, S.; Jacob, J.; Kim, J. Y.; Yang, C. *Chem. Eur. J.* **2011**, 17, 14681-14688.

[39] Zhao, X.; Zhan, X. *Chem. Soc. Rev.* **2011**, 40, 3728-3743.

[40] Liu, Y.; Ma, H.; Jen, A. K. Y. *Chem. Mater.* **1999**, 11, 27-29.

[41] Tomar, M.; Lucas, N. T.; Gardiner, M. G.; Müllen, K.; Jacob, J. *Tetrahedron Lett.* **2012**, 53, 285-288.

[42] Tomar, M.; Lucas, N. T.; Müllen, K.; Jacob, J. *Tetrahedron Lett.* **2013**, 54, 5883-5885.

6. Appendixes

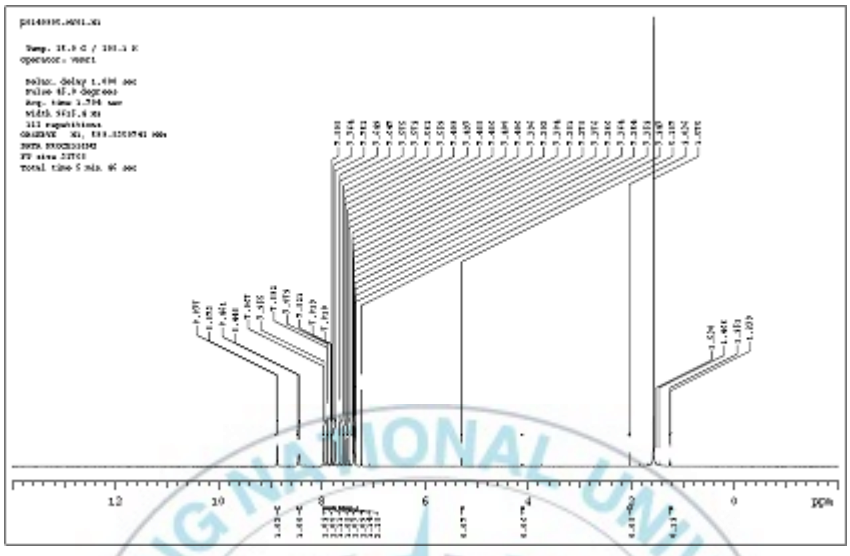

Appendix 1. ^{1}HNMR spectrum of Compound 1

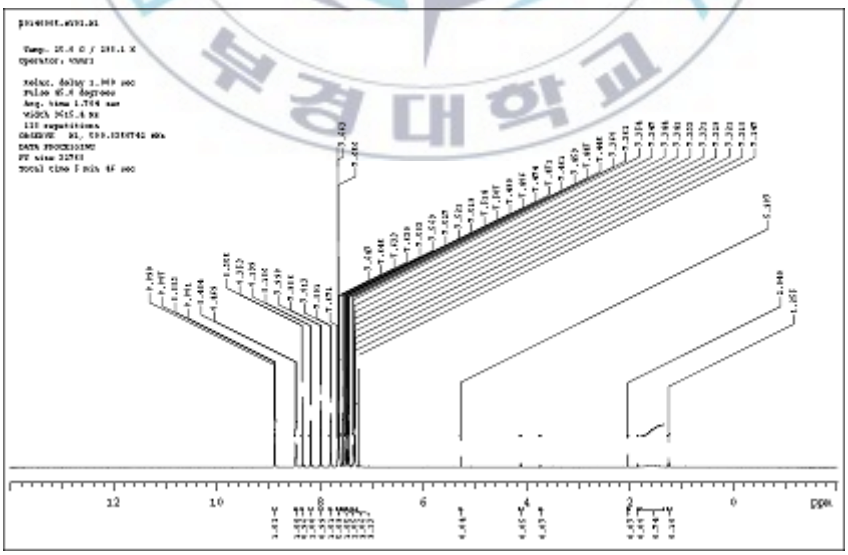

Appendix 2. ^{1}HNMR spectrum of Compound 2

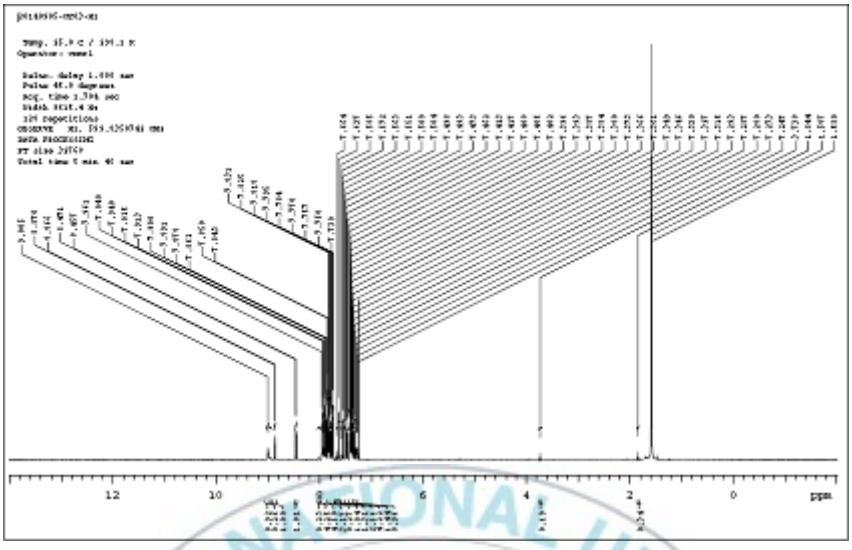

Appendix 3. ^{1}HNMR spectrum of Compound 3

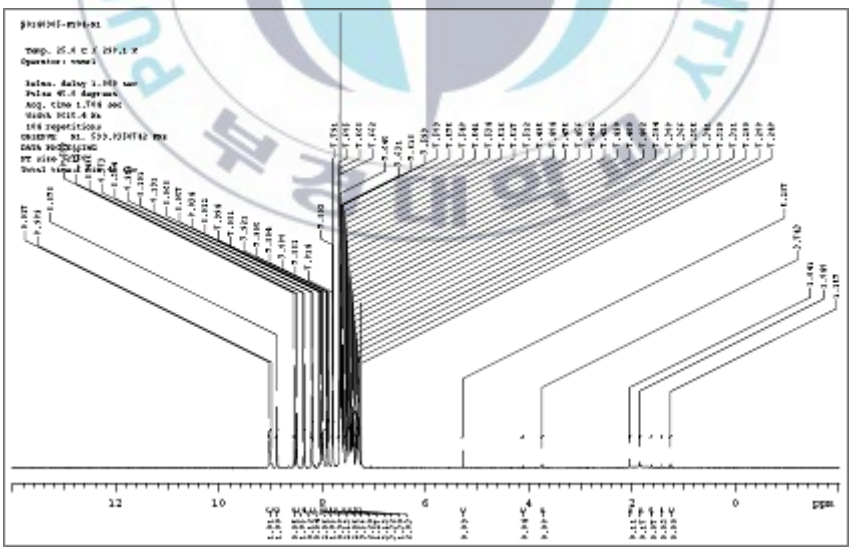

Appendix 4. ^{1}HNMR spectrum of Compound 4

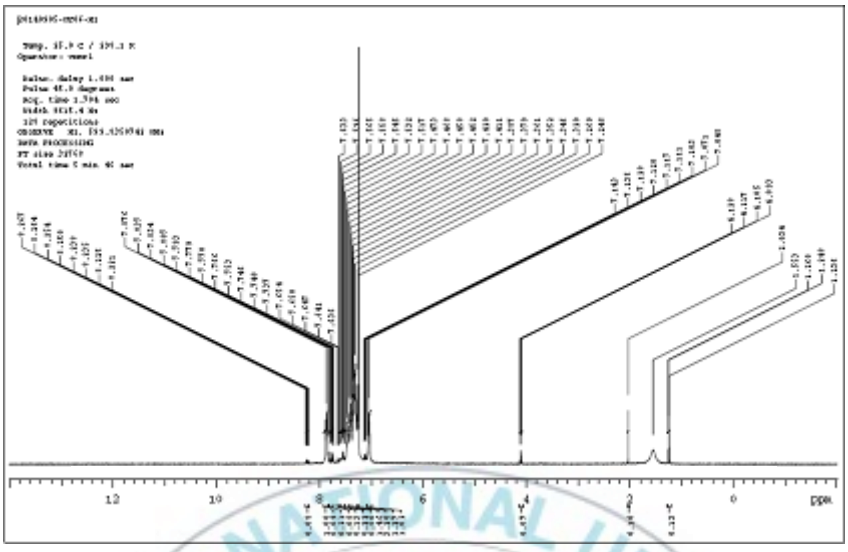

Appendix 5. ^{1}HNMR spectrum of Compound 5

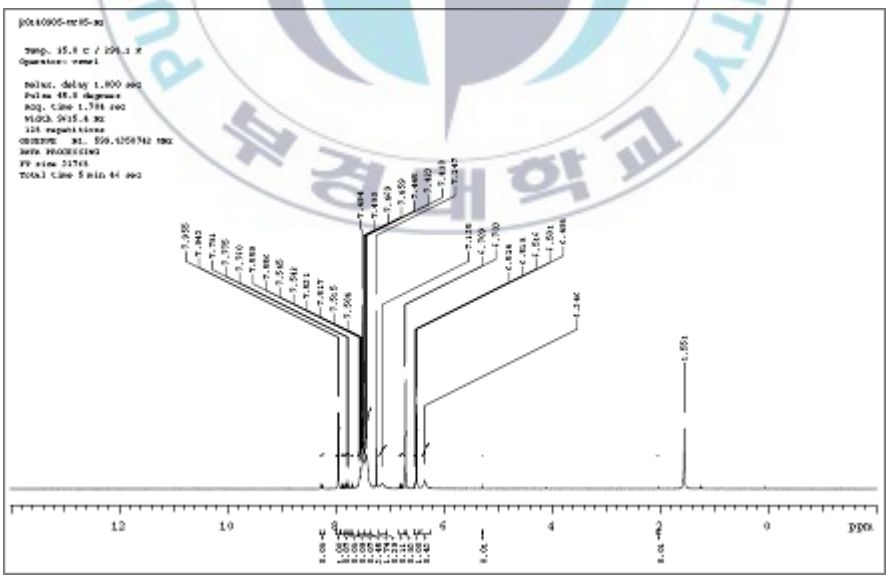

Appendix 6. ^{1}HNMR spectrum of Compound 6

Acknowledgements

First of all, I would like to express my sincere gratitude to my supervisor, Professor Se Mo Son, for his valuable advice, patient guidance and amazing support during the process of my studying in Korea. He has been providing a large amount of knowledge, the direction and skill of research, and strong motivation for my researching. His kindness, insight and continuous supports helped and encouraged me to carry on my study properly and accomplish this thesis scientifically.

I would like to thank the appraiser committee members of my thesis, Professor Jong Su Kim and Professor Sang Nam Lee, for their helpful comments and suggestions for my thesis.

I warmly appreciate all members of Printing Plate Making laboratory for their cooperation and all kindness and friendship. I am grateful that they were eager to help me in my daily life when I came to this lab.

Finally, I would like to thank to my parents, my wife, and all my close relatives for their love, encouragement and support not only in the thesis time but also in the whole of my life. Thanks to all my friends who live in Busan, Korea without their unwavering encouragement throughout my graduate studies, this thesis would not have been possible.